AMT31 Cruise Report.

RRS James Cook (JC272).

27 November to 30 December 2024.

Principal Scientist: Gavin Tilstone,

Plymouth Marine Laboratory, UK.

PML | Plymouth Marine Laboratory

Contents.

Overview.

The 31st AMT cruise departed Southampton on the 27th November 2024 and arrived in Montevideo, Uruguay on 30th December 2024. Onboard were teams from Plymouth Marine Laboratory, UK; the University of East Anglia, UK; University of Galway, Ireland; University of Rio Grande, FURG, Brazil; Alfred Wegner Institute, Germany and the University of Connecticut, USA. Operations onboard included the measurement of core AMT variables in the maintenance of a 31 year time series; 30 days of continuous underway Optical and atmospheric observations in support of the European Space Agency Sentinel satellite and the new NASA PACE satellite; Deployment of 12 autonomous argo floats for WHOI and the UK MetOffice; and between 90 and 135 samples taken for the quantification of genetic biodiversity, phytoplankton community structure and ocean acidification parameters. AMT's oceanography training programme continued with opportunities provided by POGO in the sponsorship of a research fellow from Brazil. The whole of the scientific complement would like to extend their gratitude to Captain John and his officers and crew who supported our activities throughout with dedication and extreme professionalism. Our thanks are also extended to Mark Maltby from NMF. who ensured the delivery of all scientific activities. My particular thanks to Andy Rees and Meryl Hopper who assisted in the pre-cruise logistics.

AMT is a multidisciplinary program which undertakes biological, chemical and physical oceanographic research during an annual voyage throughout the Atlantic Ocean. AMT objectives have evolved to enable the maintenance of a continuous set of observations, whilst addressing global issues that are raised throughout the most recent IPCC assessment and UK environmental strategy. AMT objectives are to:

(1) quantify the nature and causes of ecological and biogeochemical variability in planktonic ecosystems;

(2) quantify the effects of this variability on nutrient cycling, on biogenic export and on air-sea exchange of climate active gases;

(3) construct a multi-decadal, multidisciplinary ocean time-series which is integrated within a wider "Pole-to-pole" observatory concept;

(4) provide essential sea-truth validation for current and next generation satellite missions;

(5) provide essential data for global ecosystem model development and validation and;

(6) provide a valuable, highly sought after training arena for the next generation of UK and International oceanographers.

Dr. G.H. Tilstone,

Plymouth Marine Laboratory, UK. December 2024.

Cruise Participants.

Gavin Tilstone
PSO & Optics

Bethany Wilkinson
Carbonate Chemistry

Tom Jordan
Optics

Rafael Mendes
HPLC & phytoplankton

Jan Kaiser
CO2 isotopologues

Peter Croot
CDOM

Raul Costa
HPLC & phytoplankton

Xavier Warren
Optics

Francielle N. de L. Holtz Santos
POGO Fellow (eDNA)

AMT31 Cruise Participants (less Beth).

NMF Personnel.

AMT31 NMF Technician, Mark Maltby.

List of Figures and Tables.

Continuous measurements of Sea Surface Skin Temperature from Infrared Sea surface temperature Autonomous Radiometer.

Werenfrid Wimmer, University of Southampton (w.wimmer@soton.ac.uk).

Objectives:

1. Collect SI traceable SSTskin measurements for the validation of SLSTR on the ESA Sentinel 3 satellite.
2. Collect the necessary ancillary measurements for the SSTskin record to help the interpretation of the validation results. Extend the ISAR SSTskin record geographically to cover a wider range of oceanographic regimes.
3. Collect met data from the ship underway system for comparison and the complement the SSTskin data set.

Automated collection of SSTskin and meteorological data.

SSTskin data was collected by ISAR (Infrared Sea surface temperature Autonomous Radiometer) mounted on the star board side of the Metrological Platform (MP) at a 90 degree angle relative to the ships center line. The data was logged with a data logger based in the Met Lab connected to the ships network allowing for frequent data quality checks. The ancillary sensors, a Kipp and Zonen CM11, a Eppley PIR were mounted above the ISAR on the MP and a Gill Windmaster was mounted near the centre forward part of the MP in order to be free of obstruction for the Gill Windmaster, and to have a clean view of the sky for the CM11 and the PIR. The CM11 and the PIR were mounted on individual gimbals to ensure that the sensors axis is vertical even when the ship moves. The data were logged with the same logger as the ISAR data. The PIR data is processed as described in Fairall et. al. 1998. Air temperature and Humidity data were collected with a Vaisala HMP243 sensor on the port side of the monkey island with a separate data logger which was located on the bridge.

References:

Donlon, C. J. and Nightingale, T. J. (2000); Effect of Atmospheric Radiance Errors in Radiometric Sea-Surface Skin Temperature Measurements; Appl. Opt.; 39: pp. 2387–2392.

Donlon ,CJ., I. Robinson, M. Reynolds, W. Wimmer, G. Fisher, R. Edwards, and T. Nightingale, 2008: An infrared sea surface temperature autonomous radiometer (ISAR) for deployment aboard volunteer observing ships (VOS). J. Atmos. Oceanic Technol., 25, 93–113, doi:10.1175/2007JTECHO505.1.

Donlon ,CJ., W. Wimmer, I. Robinson, G. Fisher, M. Ferlet, T. Nightingale, and B. Bras, 2014: A second-generation blackbody system for the calibration and verification of sea- going infrared radiometers. J. Atmos. Oceanic Technol., 31, 1104–1127, doi:10.1175/JTECH-D-13-00151.1.

Wimmer, W., I. Robinson, and C. Donlon, 2012: Long-term validation of AATSR SST data products using shipborne radiometry in the Bay of Biscay and English Channel. Remote Sens. Environ., 116, 17–31, doi:10.1016/j.rse.2011.03.022.

Fairall, C. W., Persson, P. O. G., Bradley, E. F., Payne, R. E. and Anderson, S. P. (1998); A newlook at calibration and use of Eppley Precision Infrared Radiometers. PartI: theory and application; J. Atmos. Oceanic Technol.; 15: pp. 1229 – 1242.

Continuous measurements of partial pressure of CO2 in seawater.

Ian Brown (ib@pml.ac.uk) *Plymouth Marine Laboratory, United Kingdom*.

Rationale and Method

These measurements will contribute to our understanding of the distribution of C sources and sinks in the Atlantic Ocean and the capacity of the ocean to take up anthropogenic CO2. Underway surface measurements of CO2 partial pressure (pCO2) were measured with the PML, Live-pCO2 system. The system encompasses a non-dispersive infrared detector (LiCor, Li840), showerhead equilibrator (vented through a parallel second equilibrator), Peltier dryer, gas-sampling and electronics hardware (Kitidis et al. 2017). The system was connected to the underway-seawater flow and set up to sample every 20 min. The intake of the ship's underway-seawater system is located at approximately 7 m depth for all three ships. The LivepCO2 system was calibrated using secondary CO2 standards every hour (BOC gases Ltd; nominal 0, 250 and 450 ppmv CO2 in synthetic air). In turn, these were calibrated against NOAAcertified primary reference standards (National Oceanic and Atmospheric Administration; 244.9 and 444.4 ppmv).

Reference.

Kitidis et al. (2017) Surface ocean carbon dioxide during the Atlantic Meridional Transect (1995–2013); evidence of ocean acidification. *Progr. Oceanogr.* 158, 65-75.

Figure *1*: PML, Live-pCO2 system set-up in the deck lab on *RRS James Cook*.

Carbonate System: Total Alkalinity (TA) and pH and Sample collection for Dissolved Inorganic Carbon (DIC).

Bethany Wilkinson, Plymouth Marine Laboratory, PL1 3DH, UK, (bwi@pml.ac.uk).

Objectives.

Dissolved CO2 reacts with water to form carbonic acid (H2CO3). H2CO3 dissociates to bicarbonate (HCO3 -) and carbonate (CO3 2-) with the concomitant release of H+ , causing a reduction in pH (Dickson et al. 2007). Total alkalinity (TA) of seawater describes the sum of the concentrations of anions and defines the capacity of seawater to neutralise acid. Dissolved Inorganic Carbon is defined as the sum of all carbonate system species in seawater DIC= H2CO3+HCO3 - , CO3 2- . The objective of this work was to collect samples for the determination of TA and DIC in seawater.

Dissolved CO2 reacts with water to form carbonic acid (H2CO3). H2CO3 dissociates to bicarbonate (HCO3 -) and carbonate (CO3 2-) with the concomitant release of H+ , causing a reduction in pH. Total alkalinity (AT) of seawater describes the sum of all ionic charges in seawater, including HCO3 - , CO3 2- , H + , inorganic and organic ions. Samples for the determination of AT and pHT (measured on the total scale) were collected in order to constrain the carbonate system along the cruise track.

Methods.

The tables below list all samples collected on the underway system. Samples were collected in 125 mL borosilicate glass bottles with glass stoppers and preserved with $HgCl_2$ until analysis at PML. These samples will be analysed after the cruise. Provisional results samples will be analysed at the Plymouth Marine Laboratory after the cruise to determine DIC and TA.

The pHT method employed here has typical precision in the low 10^{-3} to 10^{-4} pH-unit range. Samples were collected in 500 mL amber glass bottles and placed in a water bath at 25 ^{o}C. pHT was determined spectrophotometrically using the m-cresol-purple dye (Dickson et al., 2007). The dye has two absorbance maxima at 434 nm and 578 nm, the ratio of which is pH-, T- and salinity-dependent. Absorbance measurements of the seawater blank, and following addition of dye (100 µL of a 2 mmol L^{-1} solution), were carried out on a Perkin Elmer, lamda 35 spectrophotometer. The temperature of the sample was recorded in the spectrophotometer cell with a NIST-traceable thermometer. pHT measurements were corrected for the pHT change due to the addition of dye according to Dickson et al. (2007). Carbonate chemistry samples collected from the underway seawater supply on AMT31 are given in Appendix 1.

References.

Dickson, A. G., C. L. Sabine, and J. R. Christion. 2007. Guide to best practices for ocean CO2 measurements. PICES Special Publication 3, p. 191. PICES Special Publication 3.

Atmospheric carbon dioxide (CO_2) polyisotopologue measurements

Jan Kaiser (J.Kaiser@uea.ac.uk) *University of East Anglia, Centre for Ocean and Atmospheric Sciences, School of Environmental Sciences, Norwich, NR4 7TJ, UK.*

Objectives

Carbon dioxide (CO_2) polyisotopologue budgets allow estimating global gross primary productivity but require leaf and soil water isotope ratios and isotopic fractionations associated with transport, release and uptake. Simultaneous measurements of $\delta(^{18}O)$ and $\delta(^{17}O)$ simplify these requirements since $\delta(^{17}O)$ variations are correlated with $\delta(^{18}O)$. The deviation of $\delta(^{17}O)$ from a mass-dependent correlation with $\delta(^{18}O)$ is expressed as the 'triple oxygen isotope excess', $\Delta(^{17}O)$. Three-dimensional modelling of atmosphere-biosphere exchange and transport of CO_2 has predicted $\Delta(^{17}O)$ to be 0.03 ‰ (30 ppm) higher in the southern than in the northern hemisphere (Koren et al., 2019). Our objective during the AMT31 cruise was to measure this interhemispheric gradient, as well as changes in CO_2 amount fraction, $y(CO_2)$, and the $^{13}C/^{12}C$ isotope delta, $\delta(^{13}C)$.

Method

We define polyisotopic elements as elements with more than one minor isotope (e.g., ^{17}O and ^{18}O next to the most abundant ^{16}O). The Natural Environment Research Council (NERC)-funded project POLYGRAM (POLYisotopologues of GReenhouse gases: Analysis and Modelling; https://polygram.ac.uk) makes targeted observations of CO_2 polyisotopologues to quantify and analyse their meridional and temporal variations, as well as characterise source fingerprints.

Figure 2: Marine air inlet at the bow meteorological platform (18.3 m above sea level)

We installed a tuneable infrared laser direct absorption spectrometer (Aerodyne TILDAS-FD-L2) in the Constant Temperature Laboratory (CT Lab) of the ship. Marine air from the 3/8 inch Synflex inlet line (Figure 2) of the General Oceanics $p(CO_2)$ system was routed from the adjacent Chemistry Lab and pumped with a KNF single-stage diaphragm pump (KNF PM2890-86, serial no. 2.17941695) through a series of filters and chillers to remove particles and atmospheric water vapour before admitted to the Aerodyne sample inlet system:

1) 40 µm filter before diaphragm pump
2) 7 µm filter after diaphragm pump
3) M&C EC30C switching chiller (–30 °C)
4) Alicat Scientific mass-flow controller (300 cm^3 min^{-1}; STP: 25 °C, 1013 mbar)
5) SP FTS VT255 vapour trap (–50 °C)
6) Overflow tee union with vent tubing (to prevent aspiration of room air)
7) 2 µm filter before Aerodyne sample inlet system

To reduce CO_2 background levels, the Aerodyne optics boxed was purged with 5 dm^3 min^{-1} (STP; controlled by Alicat Scientific mass-flow controller) of O_2 and CO_2-free N_2 from a Parker nitrogen generator (HPN2-5000C-E; serial no. 21GL0027). Two lasers measured the absorption of four CO_2 isotopologues ($^{12}C^{16}O_2$, $^{12}C^{18}O^{16}O$, $^{12}C^{17}O^{16}O$, $^{13}C^{16}O_2$) in a 36.4 m absorption cell held at 54 mbar (296.8 K). An Agilent IDP-7 scroll pump was used to evacuate the sample inlet system. The sample inlet system used pneumatic valves operated with compressed air from a cylinder (BOC, zero grade, size L; outlet: 7 bar) in the ship's gas store. Working reference, target tank and calibration standard cylinders (Luxfer) were mounted in the CT Lab to avoid thermal gradients and associated isotopic fractionation (Figure 3).

Figure 3: Aerodyne TILDAS CO_2 isotopologue measurement and gas handling system in the Constant Temperature Laboratory aboard RRS James Cook.

Sample air and a working reference were alternated every 120 s, consisting of 33 s of evacuation and refilling of the absorption cell and an 87 s-measurement interval. Raw individual isotopologue concentrations were obtained every second and used to derive raw isotope ratios. The raw sample isotope ratios were then averaged over the 87 s-measurement interval and turned into raw sample isotope deltas by using the corresponding preceding and following raw working reference isotope ratio.

Preliminary results

Average temperature and relative humidity in the CT Lab were (16.2±0.8) ºC and (68±3) %, respectively (Figure 4). Regular oscillations occurred at 3 hour-intervals, as well as at approximately 24 hour-intervals for part of the cruise. These were deemed to be small enough not to affect measurement accuracy and precision.

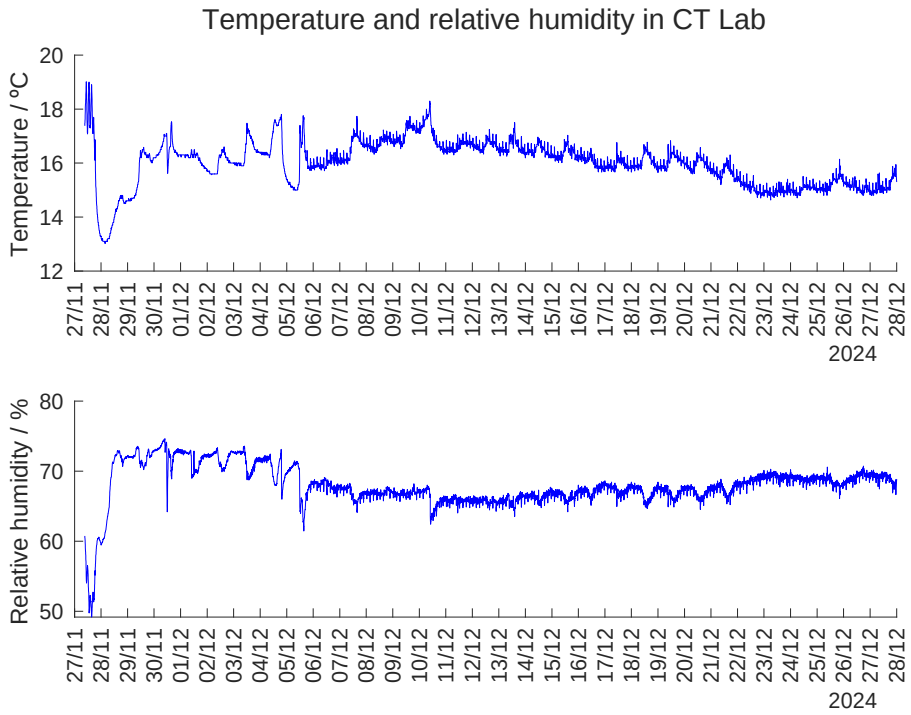

Figure 4: Temperature and relative humidity (5 min averages) in the CT Lab. Data from jcnetapp.jamescook.ad.noc.ac.uk/current_cruise/Ship_Systems/Data/TechSAS/NMEAe/temp

Ship motion was found to adversely affect data precision and, in case, of $\Delta(^{17}O)$, accuracy. However, after averaging over hourly intervals, precisions better than 0.05 µmol mol^{-1} for $y(CO_2)$, 0.01 ‰ for $\delta(^{13}C)$ and 0.03 ‰ for $\delta(^{18}O)$ were achieved, more than sufficient to resolve environmental variability (Figure 5). Day-to-day variability of target tank measurements were of the same magnitude. For $\Delta(^{17}O)$, hourly precision was better than 10 ppm (0.01 ‰), but unfortunately, the target tank measurements showed unresolved day-to-variability of the order of 40 ppm, which makes establishing the desired interhemispheric gradient more challenging. However, we are hopeful that this primary objective can still be achieved with more sophisticated data processing and correction.

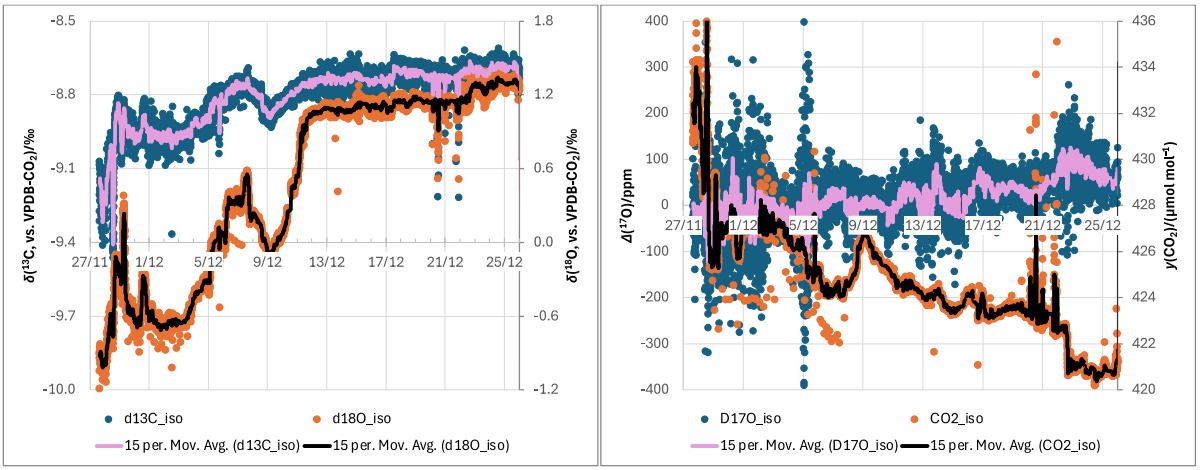

Figure 5: $\delta(^{13}C)$, $\delta(^{18}O)$, $\Delta(^{17}O)$ and amount fraction variations in atmospheric CO_2, with 1 hour moving averages. δ values are derived from raw measurements using the isotopologue method (Steur et al., 2021; Griffith, 2018) and expressed relative to the international standard VPDB-CO_2.

References

Griffith, D. W. T.: Calibration of isotopologue-specific optical trace gas analysers: a practical guide, Atmos. Meas. Tech., 11, 6189-6201, 10.5194/amt-11-6189-2018, 2018.

Koren, G., Schneider, L., van der Velde, I. R., van Schaik, E., Gromov, S. S., Adnew, G. A., Mrozek Martino, D. J., Hofmann, M. E. G., Liang, M.-C., Mahata, S., Bergamaschi, P., van der Laan-Luijkx, I. T., Krol, M. C., Röckmann, T., and Peters, W.: Global 3-D simulations of the triple oxygen isotope signature $\Delta^{17}O$ in atmospheric CO_2, J. Geophys. Res., 124, 8808-8836, 10.1029/2019JD030387, 2019.

Steur, P. M., Scheeren, H. A., Nelson, D. D., McManus, J. B., and Meijer, H. A. J.: Simultaneous measurement of $\delta^{13}C$, $\delta^{18}O$ and $\delta^{17}O$ of atmospheric CO_2 – Performance assessment of a dual-laser absorption spectrometer, Atmos. Meas. Tech., 14, 4279-4304, 10.5194/amt-14-4279-2021, 2021.

Aerosol sampling for trace metal, soluble ion and organic matter concentration analyses

Jan Kaiser (J.Kaiser@uea.ac.uk), Alex Baker (Alex.Baker@uea.ac.uk, not on board), University of East Anglia, Centre for Ocean and Atmospheric Sciences, School of Environmental Sciences, Norwich, NR4 7TJ, UK

Objectives

Trace elements, such as iron, are often scarce in surface waters of the ocean and in some cases their availability limits rates of phytoplankton growth or nitrogen fixation. The atmospheric transport of these trace elements to the remote ocean in atmospheric particles (aerosol) therefore plays an important role in regulating the primary productivity of the oceans. Aerosol transport is highly variable in space and time, and it is nearly impossible to directly measure particle deposition to the ocean. This makes it difficult to assess the impact of particle deposition, and the micronutrients deposited with it, on ocean biogeochemistry.

Method / Work at sea

A high-volume aerosol collector was installed on the top of the wheelhouse ("monkey island"). The deck is 18.9 m above sea level. The top of the collector hatch was 1.1 m above deck level (20.0 m above sea level). Wind speed and direction were continuously monitored by an automated wind sector controller (WSC; Campbell Scientific CR800 datalogger), connected to a Gill WindSonic 1405 (Option 1) sonic anemometer (1.3 m above deck level; 20.2 m above sea level). The WSC automatically switched off the pump in the aerosol collector when the wind speed was less than 2 m s^{-1} or from a bearing between 150º and 280º, relative to the ship's bow. In this way, sampling of emissions from the ship's stack was avoided. The collector was installed 5 m aft and 4 m starboard of the anemometer (Figure 6).

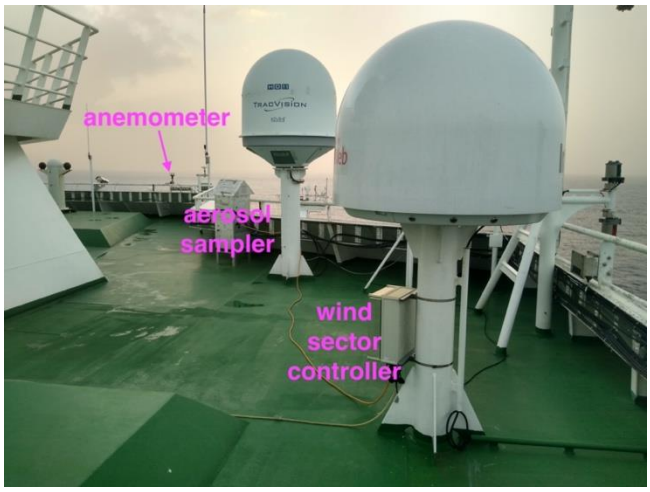

Figure 6: Aerosol sampling equipment configuration on the top of the wheelhouse

The collector was equipped with a total suspended particulate sampling head. The pump produced an air volume flow of approximately 1 m^3 min^{-1}. Samples were collected on acid-washed Whatman 41 cellulose filters, which were exposed on the aerosol collector for 24 to 48 h. Active pumping times varied between 1.66 and 26.75 hours. The filter cassettes were changed in a laminar flow hood (Bassaire K3V; installed in the ship's Main Lab), which was turned on 10 minutes prior to any operations. Filters were stored in a -20 ºC freezer. They will be shipped back frozen to the University of East Anglia for trace metal, soluble ion and organic substance analyses. Aerosol concentrations will be calculated from the amounts of substance

on the filters and the total air sampling volumes. Air-sea fluxes can then be estimated from wind-speed based deposition velocity estimates.

Preliminary results

Aerosol collection periods are summarized in Table 1.

Sample 5 (AMT31TM05) may have been contaminated with white paint flakes from ship due to the high wind speeds during its collection period. Paint flakes were found under the hatch of the sampler.

Samples 10 and 11 (from between 20º N and 9º N) were covered thick in orange-brown dust, presumably from the Saharan desert.). The particle load was so high that it was loose on the filter paper. Hazy skies prevailed because of the high dust aerosol concentration.

Samples 12 to 14 (from between 9º N and 8º S) were coloured light beige or grey, perhaps indicative of soot from biomass burning.

The anemometer was initially mounted on a wooden pole on the starboard side rail of the "monkey island", but the attachment clamp was too loose, allowing the anemometer to rotate 30º towards starboard. When this problem was discovered on 5 December 2024, the anemometer was moved and attached directly to the forward rail of the "monkey island" (Figure 7).

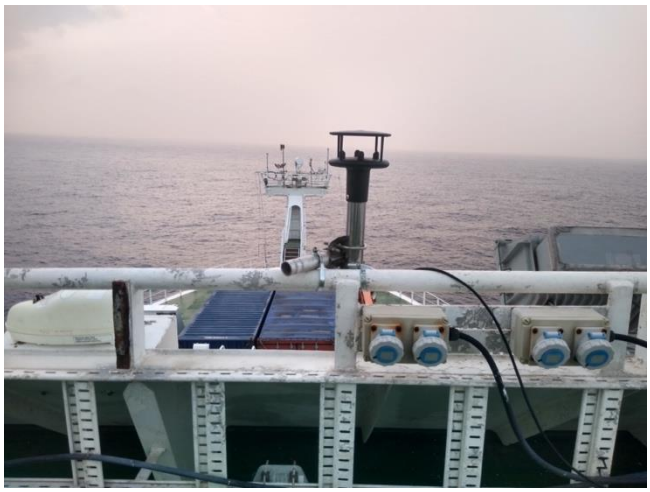

Figure 7: Installation of sonic anemometer on forward rail of the ship's "monkey island"

Active pumping times between 1 and 12 December 2024 were significantly lower than the filter exposure times due to the prevailing relative wind direction (270º to 300º) from aft or port side of the ship. It was initially unclear whether this was indeed due to the wind direction because the red "Program Status" LED on the WSC logger had stopped flashing on 5 or 6 December (a flash every 15 seconds indicates the control programme is running). This could have indicated a "hung" WSC logger, and a restart and reinstallation of the logger programme were considered. However, since the disc chart indicated that the pump motor was still being turned on and off for periods of time, the logger programme was deemed to be running and controlling the pump as intended. No further action was taken and the WSC logger appeared to operate as intended until end of the cruise (with the "Program Status" LED permanently off).

Samples 18 to 20, 22 and 23 were also affected by unfavourable wind direction and/or speed (Figure 8; Table 1). For Sample 21, the pump ran the full 45 hours of the filter mounted on the cassette, but at the end of the sampling period, it was noted that the large motor mounting thread was loose, which may have reduced the flow over the filter without affecting the flow recorded on the chart. The fitting was retightened before starting sample 22.

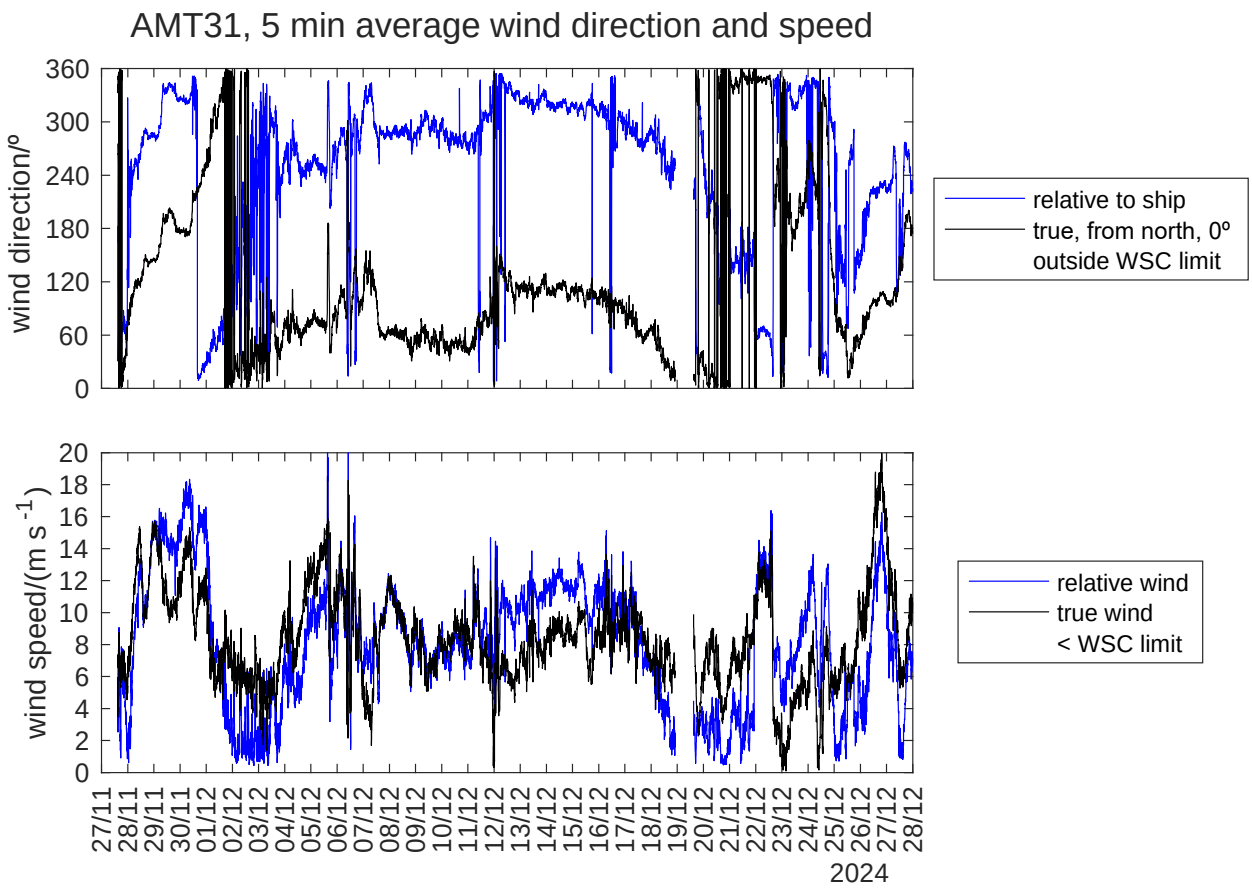

Figure *8*: Relative and true wind speed and direction as a function of time as well as the thresholds for turning on the motor (relative wind speed >2 m s^{-1} or relative wind direction outside the 150º to 280º sector with respect to the bow of the ship).

Table 1: Aerosol collection periods during AMT31 (JC 272) with pump motor operation times, Δ*t*(pump), and cassette times, Δ*t*(cassette)

Sample ID	Start	UTC	Lat. º N	Long. º W	End	UTC	Lat. º N	Long. º W	Δ*t*(pump) h	Δ*t*(cassette) h	Notes
AMT31TM01	27/11/24	11:40	50.892	1.395	28/11/24	11:40	49.533	5.667		24.00	cassette blank
AMT31TM02	28/11/24	12:00	49.517	5.733	28/11/24	12:05	49.517	5.733	<0.01	0.08	motor blank
AMT31TM03	28/11/24	12:10	49.483	5.783	29/11/24	12:10	47.717	10.367	0.00	24.00	exposure blank
AMT31TM04										0.00	filter blank (punctured)
AMT31TM05	29/11/24	12:25	47.667	10.433	30/11/24	16:20	44.814	14.483	24.99	27.92	white paint flakes
AMT31TM06	30/11/24	16:38	44.900	14.500	01/12/24	16:10	41.450	16.900	23.56	23.53	
AMT31TM07	01/12/24	16:28	41.400	16.933	03/12/24	16:16	33.867	21.717	11.66	47.80	
AMT31TM08	03/12/24	16:36	33.833	21.733	05/12/24	17:10	26.400	26.233	1.66	48.57	
AMT31TM09	05/12/24	17:30	26.367	26.250	07/12/24	11:30	20.467	29.733	16.91	42.00	grey dust
AMT31TM10	07/12/24	11:50	20.417	29.767	08/12/24	19:05	15.450	28.833	13.40	31.25	orange-brown dust
AMT31TM11	08/12/24	19:20	15.417	28.817	10/12/24	08:00	9.350	27.300	26.75	36.67	orange-brown dust
AMT31TM12	10/12/24	08:18	9.300	27.283	11/12/24	19:25	4.167	26.017	13.11	35.12	light beige dust
AMT31TM13	11/12/24	19:42	4.117	26.017	12/12/24	19:18	0.650	25.150	23.59	23.60	light grey dust
AMT31TM14	12/12/24	19:33	0.617	25.150	13/12/24	19:33	-3.467	25.000	24.00	24.00	light grey dust
AMT31TM15	13/12/24	19:44	–3.500	25.000	14/12/24	19:44	–7.650	25.000	24.00	24.00	light grey dust
AMT31TM16	14/12/24	19:58	–7.683	25.000	15/12/24	19:58	–11.833	25.000	24.00	24.00	
AMT31TM17	15/12/24	20:10	–11.867	25.000	16/12/24	20:05	–15.183	25.000	21.74	23.92	
AMT31TM18	16/12/24	20:16	–15.217	25.000	18/12/24	20:16	–22.950	25.000	10.64	48.00	
AMT31TM19	18/12/24	20:26	–22.983	25.000	20/12/24	20:15	–31.000	25.000	11.99	47.82	
AMT31TM20	20/12/24	20:25	-31.017	25.000	22/12/24	20:25	-35.550	28.950	21.66	48.00	
AMT31TM21	22/12/24	20:35	-35.550	29.000	24/12/24	17:35	-36.750	37.867	45.00	45.00	tightened motor thread
AMT31TM22	24/12/24	17:50	-36.750	37.917	26/12/24	17:35	-39.000	46.800	6.35	47.75	
AMT31TM23	26/12/24	17:50	-39.017	46.850	28/12/24	22:50	-38.233	51.667	0.00	29.00	“exposure blank”

Continuous measurements of surface inherent and apparent optical properties.

Tom Jordan (tjor@pml.ac.uk), Gavin Tilstone (ghti@pml.ac.uk), Plymouth Marine Laboratory, UK.

Objectives.

The objective of the optics work on AMT 31 was to determine surface inherent (absorption, scattering, beam attenuation) and apparent (remote-sensing reflectance) optical properties in support of satellite calibration/validation. AMT 31 is the first AMT cruise where the NASA PACE satellite - with hyperspectral sensor OCI - has been in orbit. Additionally, in conjunction with the discrete samples on the cruise, the continuous optics data supports algorithm development for phytoplankton community structure and colour dissolved organic matter (CDOM).

Inherent optical properties were measured using a semi-autonomous flow-through system, (Dall Olmo *et al.* 2009). Hyperspectral absorption and beam attenuation were measured on the wavelength range 400-750 nm using a Seabird AC-S system. The particulate components of absorption, scattering, and beam attenuation were derived via hourly measurement sequences of filtered (0.2 micron) and bulk intervals. Total Chlorophyll-a concentrations were then derived from the particulate absorption using the line-height method (Brewin et al. 2016). The CDOM absorption component was derived at an hourly resolution, by differencing the absorption measurements during filtered intervals and an ultrapure baseline (Dall Olmo *et al.* 2017).

The flow-through data were collected near-continuously along the cruise track between 28th November and 27th December 2024 (Figure 9). The particulate data were processed at 1-minute binning with uncertainty estimates for each optical variable, following Jordan *et al.* 2024. The output data files include the ships' underway data, and salinity and temperature measurements made within the optical flow- though system.

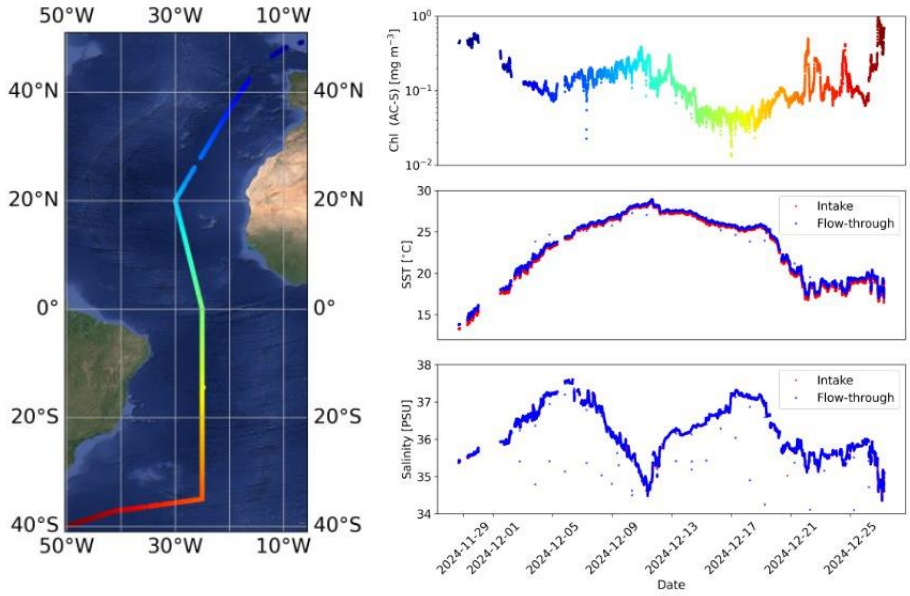

Figure 9. Left panel: Data coverage from the flow-through inherent optical properties system . Right panel: Total Chlorophyll-a (derived from particulate absorption), Sea surface temperature, and salinity along the cruise transect. The Total Chlorophyll-a line colour matches the coverage map locations).

Above-water radiometric measurements were taken continuously during daylight hours using a Satlantic HyperSAS system consisting of three 136-channel HyperOCR radiometers (wavelength range approximately 350-800 nm). Remote-sensing reflectance was then derived from near-synchronous HyperOCR measurements of water-leaving radiance, sky radiance, and downwelling irradiance. The reflectance data were processed with uncertainties using the open-source HyperCP community processor (Aurin et al. 2024), following a processing configuration based on past AMT cruises (Lin et al. 2023). High-quality reflectance data were collected dalily in 3-6 hour intervals from 7th December onwards (Figure 10). Before this date, the measurement geometry (solar elevation and azimuth) was unsuitable.

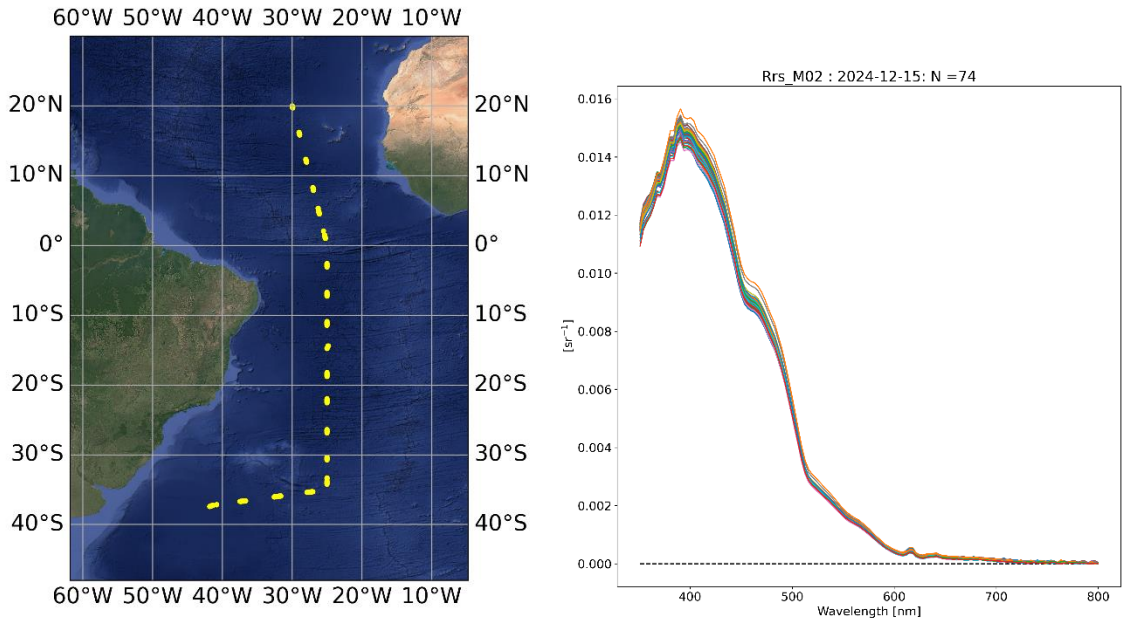

Figure 10. Left panel: Coverage of reflectance data passing initial quality control from HyperSAS radiometry system from 7th-25th Dec (excluding final 2 days of data collection). Right panel: Example reflectance spectra from 15th Dec 2024.

References

Aurin, D. et al. (2024). HyperInSPACE Community Processor (HyperCP), accessible online, https://github.com/nasa/HyperCP

Brewin,RW. et al. (2016) Underway spectrophotometry along the Atlantic Meridional Transect reveals high performance in satellite chlorophyll retrievals, Remote Sensing of Environment, 183, 82-97.

Dall'Olmo G. et al. (2009). Significant contribution of large particles to optical backscattering in the open ocean. Biogeosciences, 6, 947–967.

Dall'Olmo, G. et al. (2017). "Determination of the absorption coefficient of chromophoric dissolved organic matter from underway spectrophotometry," Opt. Express 25, A1079-A1095 (2017)

Lin et al. (2023), "Derivation of uncertainty budgets for continuous above-water radiometric measurements along an Atlantic Meridional Transect," Opt. Express 30, 45648-45675.

Jordan, T.M. et al., (2024). A compilation of surface inherent optical properties and phytoplankton pigment concentrations from the Atlantic Meridional Transect. Earth Syst. Sci. Data Discuss., 2024: 1-33.

Measurement of Hyperspectral Backscatter and Particle Size Distribution.

Xavier Warren (warren_javierj@gmail.com), University of Connecticut, USA.

Objectives

Determine both size distribution and hyperspectral backscatter of particles in surface level waters to support *in situ* AOP measurements, as well as assist in satellite validation and calibration methods, primarily with the NASA PACE satellite. Cooperatively, with other, on-board IOP measurements, hyperspectral backscatter and particle size distribution provide additional insight into particle types and dynamics in surface level waters across the transect.

Methods

Hyperspectral Backscatter

Hyperspectral backscatter measurements were obtained through a continuous flow-through system developed by Sequoia Scientific measured in the wavelength range of 430-700 nm at a resolution of 10 nm. Particle backscatter coefficients were derived using the methodology described in Sullivan et al. (2012) and Boss et al. (2001). Measurement remained continuous for 22 hours/day for the duration of the cruise (November 28th - December 27th); collection was paused between 0700-0900 UTC to offload data and clean/calibrate the instrument. Data was processed into one-minute bins for simplified integration with other IOP, flowthrough products collected during the cruise (Jordan et al. 2024). Output files will reflect the particulate backscatter coefficient at each wavelength interval with its standard deviation for each corresponding timestamp.

Particle Size Distribution

Particle size distribution was collected via LISST-100X, also developed by Sequoia Scientific. Discrete, surface level samples were taken every hour from 0900-1900 UTC: beginning on November 29 and continuing for the remainder of the expedition. Size distribution within the range of 1.2 to 250 microns. Additionally, surface water samples to be run in an IFCB, developed by McLane Labs, were collected. Typical IFCB sample analysis is conducted in a timely fashion, but due to scheduling constraints, samples were forced to be preserved in non-ideal conditions. Due to this, there is no certainty in the quality of IFCB measurements at the time of writing this report.

References

Boss, E., & Pegau, W. S. (2001). Relationship of light scattering at an angle in the backward direction to the backscattering coefficient. *Applied Optics*, *40*(30), 5503. https://doi.org/10.1364/ao.40.005503

Sullivan, M. et al. (2012). Measuring optical backscattering in water. *Light Scattering Reviews 7*, 189–224. https://doi.org/10.1007/978-3-642-21907-8_6

Jordan, T. et al. (2024). *A Compilation of Surface Inherent Optical Properties and Phytoplankton Pigment Concentrations from the Atlantic Meridional Transect*. https://doi.org/10.5194/essd-2024-267

Aerosol Optical Depth – Microtops II sunphotometer.

Tom Jordan, Plymouth Marine Laboratory, UK, for:

Alexander Smirnov, MARITIME AEROSOL NETWORK (MAN), NASA Goddard Space Flight Center (GSFC), USA.

Objective.

Take aerosol optical depth (AOD) measurements using a Microtops II sun photometer and contribute for the Maritime aerosol network (MAN) database (Smirnov et al. 2009).

Method.

Whenever conditions allowed (i.e. clear sky conditions) measurements were taken with a Microtops II sun photometer configured to acquired data at five channels 380, 440, 675, 870 and 936 nm. Microtops was connected to a GPS for accurate time and location logging, and while targeting the Sun, 6-10 scans were taken. Procedure was repeated with 2 min interval. Data were downloaded and sent to the MAN for processing and dissemination. Data collected during the campaign are available at: https://aeronet.gsfc.nasa.gov/new_web/cruises_new/Discovery_19_0.html.

References.

Smirnov, A., B. N. Holben, I. Slutsker, D. M. Giles, C. R. McClain, T. F. Eck, S. M. Sakerin, A. Macke, P. Croot, G. Zibordi, P. K. Quinn, J. Sciare, S. Kinne, M. Harvey, T. J. Smyth, S. Piketh, T. Zielinski, A. Proshutinsky, J. I. Goes, N. B. Nelson, P. Larouche, V. F. Radionov, P. Goloub, K. Krishna Moorthy, R. Matarrese, E. J. Robertson, and F. Jourdin (2009), Maritime Aerosol Network as a component of Aerosol Robotic Network, J. Geophys. Res.,114, D06204, doi:10.1029/2008JD011257

Phytoplankton pigments from High Performance Liquid Chromatography (HPLC) and phytoplankton species analysis by microscopy with coccolithophore counts.

Carlos Rafael Borges Mendes and Raul Costa, FURG, Brazil.

Objectives.

- To examine the surface phytoplankton pigment composition along the AMT31 transect for the continuation of a 29-year spatially extensive and internally consistent time series of observations on the pigment structure of phytoplankton in the Atlantic Ocean (NERC-NC AMT).
- To collect phytoplankton pigment data for the development and validation of remote-sensing algorithms and marine ecosystem models designed to predict and model the phytoplankton biomass and community structure at basin scales.
- To collect phytoplankton pigment data for the validation of remote-sensing algorithms for estimating phytoplankton pigment concentration on the newly-launched NASA PACE mission.
- To characterize the structure of phytoplankton communities at surface, including the coccolithophorids, by microscopy, with a taxonomic resolution at the genus and/or species level.

Methods

Phytoplankton pigments from High Performance Liquid Chromatography (HPLC)

Seawater samples were collected three times per day at 09:00, 12:00, 15:00 (UTC time) from the ship's underway system, to provide good spatial distribution along the track. Seawater was sampled into 9.5 L polypropylene carboys covered in black plastic to keep out the light. At all sampling times, 2 L of seawater were filtered under low vacuum (< 5 in. Hg) through Whatman GF/F filters (nominal pore size of 0.7 µm; 25 mm in diameter) to determine the total biomass (chlorophyll *a*; chl-*a*) and respective pigment profile (chlorophylls and carotenoids) by High Performance Liquid Chromatography (HPLC). Additionally, to complement the total phytoplankton chl-*a* biomass information, size fractionation of this biomass was performed at two times of the day (09:00 and 15:00; UTC time) in order to have a good daily representation throughout the entire transect. The fractionation was carried out by sequential filtering of water subsamples (1 L). Each sample (in duplicate) was firstly filtered using a polycarbonate filter with pore size of 10 µm (GVS Life Sciences North America, 47 mm). The collected filtrate was subsequently filtered into a polycarbonate filter with pore size of 2 µm (GVS Life Sciences North America, 47 mm). Lastly, the collected filtrate was filtered into GF/F filter (Whatman) to retain the cells between 0.7 and 2 µm. The first two filtrations were performed by gravity and the last one under low vacuum pump (< 5 in. Hg). The filtration by gravity minimizes the problems of vacuum filtration, such as breaking phytoplankton cells. This procedure will allow measuring the concentration of chl-*a* (and accessory pigments) for the picophytoplankton (between 0.7 and 2

µm), nanophytoplankton (2–10 µm), and microphytoplankton (> 10 µm) by HPLC. At the end of the filtrations (total biomass and fractionation), the vacuum was left for a few seconds in order to eliminate the exceeding water. Using appropriate tweezers, the filters were folded in two and wrapped in aluminium foil. A first label was glued inside and a second on the outer face of the aluminium wraps. The filters were then flash frozen in liquid nitrogen and stored in the - 80ºC freezer. Frozen samples will be further analysed using HPLC methods at FURG after the cruise. The sampling sheet was filled out with the chosen filtration volumes and sample information.

Coccolithophores

At the same sampling times of the fractionation, i.e., 9:00 and 15:00 (UTC time), another filtration was also performed aimed at analysing coccolithophorids. For this purpose, 4 L of seawater were filtered through mixed cellulose nitrate filters of 47 mm diameter and 0.45 µm pore size (Whatman) by means of a low-pressure vacuum (< 5 in. Hg) pump. After filtering all the volume, the filters were gently rinsed with a few drops of buffered solution (1 L Milli-Q water + 0.15 g Na_2CO_3 + 0.2 g $NaHCO_3$ = measured pH = 9-10), to remove the salt. Finally, the filters were dried at room temperature and stored in labelled petri dishes. The filtered material for coccolithophores will be used for studies on communities and coccolith species using both polarizing light and scanning electron microscopy at Faculty of Sciences of the University of Lisbon (FCUL).

Microscopy

In order to determine the species composition, at the first sampling time of each day – 9:00 (UTC time) –, i.e., once a day, water samples were preserved in amber glass flasks (100 mL) with 2% alkaline Lugol's iodine solution for phytoplankton identification and counting. Settling chambers (from 50 to100 mL settling volume) will be inspected on an Axiovert 135 ZEISS inverted microscope at 200×, 400× and1000× magnification, according to specific literature.

Table 2. HPLC and phytoplankton samples collected from the underway seawater supply on AMT31.

Data	Station	Time (UTC)	Latitude	Longitude	T (ºC)	Salinity	HPLC (total biomass)	HPLC (size fraction)	Microscopy	Coccoliths
28/11/2024	#1	09:00	49º44.430'N	004º52.321'W			✓	✓	✓	✓
	#2	12:00	49º30.275'N	005º45.174'W			✓			
	#3	15:00	49º16.362'N	006º19.748'W	13.19	35.33	✓	✓		✓
29/11/2024	#4	09:00	48º01.490'N	009º53.709'W	13.97	35.54	✓	✓	✓	✓
	#5	12:00	47º44.038'N	010º20.970'W	14.71	35.39	✓			
	#6	15:00	47º26.327'N	010º47.968'W	14.57	35.58	✓	✓		✓
30/11/2024	#7	09:00	45º40.384'N	013º27.991'W	15.64	35.69	✓	✓	✓	✓
	#8	12:00	45º23.737'N	013º52.486'W	15.73	35.68	✓			
	#9	15:00	45º05.493'N	014º19.572'W	15.84	35.66	✓	✓		✓
01/12/2024	#10	09:00	42º34.139'N	016º08.074'W	17.06	35.84	✓	✓	✓	✓
	#11	12:00	42º06.717'N	016º26.881'W	17.67	35.95	✓			
	#12	15:00	41º37.934'N	016º46.393'W	17.84	35.94	✓	✓		✓
02/12/2024	#13	09:00	38º45.020'N	018º40.318'W	18.99	36.25	✓	✓	✓	✓
	#14	12:00	38º19.822'N	018º56.703'W	19.5	36.38	✓			
	#15	15:00	37º57.181'N	019º10.924'W	20.15	36.48	✓	✓		✓
03/12/2024	#16	09:00	35º01.958'N	021º00.465'W	20.89	36.62	✓	✓	✓	✓

	#17	12:00	34º31.440'N	021º19.136'W	20.83	36.63	✓			
	#18	15:00	34º02.536'N	021º36.727'W	21.69	36.53	✓	✓		✓
04/12/2024	#19	09:00	31º12.682'N	023º18.244'W	22.72	37.16	✓	✓	✓	✓
	#20	12:00	30º45.620'N	023º34.011'W	23.07	37.17	✓			
	#21	15:00	30º18.357'N	023º49.730'W	23.17	37.23	✓	✓		✓
05/12/2024	#22	09:00	27º35.716'N	025º30.167'W	23.52	37.28	✓	✓	✓	✓
	#23	12:00	27º09.237'N	025º46.530'W	23.48	37.24	✓			
	#24	15:00	26º41.878'N	026º03.041'W	23.75	37.37	✓	✓		✓
06/12/2024	#25	09:00	24º02.953'N	027º38.204'W	24.54	37.48	✓	✓	✓	✓
	#26	12:00	23º38.149'N	027º52.807'W	25.15	37.35	✓			
	#27	15:00	23º11.733'N	028º08.454'W	25.21	37.35	✓	✓		✓
07/12/2024	#28	09:00	20º49.165'N	029º31.488'W	25.69	37.31	✓	✓	✓	✓
	#29	12:00	20º24.281'N	029º46.066'W	25.78	36.9	✓			
	#30	15:00	19º59.400'N	029º59.630'W	25.94	36.92	✓	✓		✓
08/12/2024	#31	09:00	17º05.129'N	029º14.810'W	25.82	36.71	✓	✓	✓	✓
	#32	12:00	16º36.877'N	029º07.652'W	26.12	36.47	✓			
	#33	15:00	16º07.215'N	029º00.044'W	26.3	36.2	✓	✓		✓
09/12/2024	#34	09:00	13º12.831'N	028º16.080'W	26.81	35.93	✓	✓	✓	✓
	#35	12:00	12º45.005'N	028º08.980'W	26.39	36.18	✓			
	#36	15:00	12º14.517'N	028º01.695'W	27.11	35.81	✓	✓		✓
10/12/2024	#37	09:00	09º10.320'N	027º15.492'W	27.91	35.55	✓	✓	✓	✓
	#38	12:00	08º41.810'N	027º08.393'W	28.02	35.57	✓			
	#39	15:00	08º11.553'N	027º00.843'W	28.1	35.27	✓	✓		✓
11/12/2024	#40	09:00	05º20.821'N	026º18.691'W	28.22	34.5	✓	✓	✓	✓
	#41	12:00	05º18.596'N	026º18.007'W	28.36	34.66	✓			
	#42	15:00	04º51.267'N	026º11.527'W	28.74	34.85	✓	✓		✓
12/12/2024	#43	09:00	02º11.080'N	025º32.001'W	27.32	35.86	✓	✓	✓	✓
	#44	12:00	01º49.190'N	025º26.922'W	27.2	35.96	✓			
	passage through the equator / ceremonial to Neptune									
13/12/2024	#45	09:00	01º41.685'S	025º00.092'W	27.28	36.25	✓	✓	✓	✓
	#46	12:00	02º11.187'S	024º59.989'W	27.28	36.21	✓			
	#47	15:00	02º42.510'S	024º59.996'W	27.33	36.12	✓	✓		✓
14/12/2024	#48	09:00	05º48.878'S	025º00.016'W	27.01	36.33	✓	✓	✓	✓
	#49	12:00	06º19.597'S	025º00.017'W	26.88	36.34	✓			
	#50	15:00	06º49.990'S	024º59.999'W	26.89	36.33	✓	✓		✓
15/12/2024	#51	09:00	09º57.995'S	025º00.022'W	25.98	36.55	✓	✓	✓	✓
	#52	12:00	10º28.600'S	025º00.078'W	25.97	36.6	✓			
	#53	15:00	11º00.141'S	025º00.005'W	26	36.64	✓	✓		✓
16/12/2024	#54	09:00	14º09.447'S	025º00.001'W	25.8	36.72	✓	✓	✓	✓
	#55	12:00	14º21.544'S	024º58.550'W	25.77	36.71	✓			
	Ship stopped / Deep tow cable rewind									
17/12/2024	#56	09:00	17º20.556'S	024º59.954'W	25.47	37.3	✓	✓	✓	✓
	#57	12:00	17º50.143'S	025º00.230'W	25.08	37.21	✓			
	#58	15:00	18º20.979'S	025º00.059'W	25.27	37.23	✓	✓		✓
18/12/2024	#59	09:00	21º07.922'S	024º59.943'W	25.26	37.1	✓	✓	✓	✓
	#60	12:00	21º35.361'S	025º00.085'W	25.3	37.08	✓			
	#61	15:00	22º04.641'S	025º00.032'W	25.54	37.1	✓	✓		✓
19/12/2024	#62	09:00	25º15.367'S	025º00.031'W	24.95	36.61	✓	✓	✓	✓
	#63	12:00	25º44.895'S	025º00.163'W	25.07	36.63	✓			
	#64	15:00	26º19.411'S	025º00.056'W	24.35	36.44	✓	✓		✓

20/12/2024	#65	09:00	29º29.262'S	025º00.033'W	21.54	35.75	✓	✓	✓	✓
	#66	12:00	29º57.146'S	025º00.043'W	21.12	35.69	✓			
	#67	15:00	30º21.313'S	024º59.894'W	21.41	35.82	✓	✓		✓
21/12/2024	#68	09:00	32º40.015'S	024º59.997'W	19.88	35.79	✓	✓		✓
	#69	12:00	33º07.667'S	024º59.917'W	20.24	35.95	✓			
	#70	15:00	33º41.736'S	024º59.989'W	19.75	35.79	✓	✓		✓
22/12/2024	#71	09:00	35º15.451'S	026º52.322'W	18.22	35.58	✓	✓	✓	✓
	#72	12:00	35º19.893'S	027º24.278'W	18.41	35.61	✓			
	#73	15:00	35º24.314'S	027º57.343'W	17.15	35.38	✓	✓		✓
23/12/2024	#74	09:00	35º52.742'S	0.31º25.228'W	18.39	35.55	✓	✓	✓	✓
	#75	12:00	35º57.142'S	031º58.748'W	17.93	35.53	✓			
	#76	15:00	36º01.890'S	032º32.286'W	18.34	35.63	✓	✓		✓
24/12/2024	#77	09:00	36º31.160'S	036º08.353'W	18.55	35.75	✓	✓	✓	✓
	#78	12:00	36º35.897'S	036º43.893'W	17.94	35.34	✓			
	#79	15:00	36º40.865'S	037º21.379'W	17.37	35.31	✓	✓		✓
25/12/2024	#80	09:00	37º10.788'S	041º03.102'W	18.96	35.83	✓	✓	✓	✓
	#81	12:00	37º19.199'S	041º35.034'W	18.8	35.84	✓			
	#82	16:00	37º24.505'S	041º48.733'W	19.06	35.81	✓	✓		✓
26/12/2024	#83	09:00	38º26.359'S	045º03.876'W	17.54	35.4	✓	✓	✓	✓
	#84	12:00	38º37.113'S	045º37.049'W	19.35	35.67	✓			
	#85	15:00	38º49.269'S	046º15.436'W	18.94	35.36	✓	✓		✓
	#86	21:00	39º13.718'S	047º32.557'W	16.67	34.76	✓			
27/12/2024	#87	09:00	39º59.361'S	049º56.239'W	19.54	35.91	✓	✓		✓
	#88	12:00	39º36.678'S	050º19.069'W	19.82	35.9	✓			
	#89	15:00	39º13.104'S	050º42.365'W	19.63	35.61	✓	✓	✓	✓

Discrete fluorometric analysis of chlorophyll *a*.

Francielle N. de L. Holtz Santos, POGO Fellowship currently at AWI, Germany, (fr.holtz@gmail.com) with *Bethany Wilkinson, Plymouth Marine Laboratory, PL1 3DH, UK,* (bwi@pml.ac.uk).

Cruise Objectives.

Quantification of chlorophyll-a concentrations using 20 µm, 2 µm, and 0.1 µm polycarbonate hydrophilic filters to evaluate phytoplankton size distribution for Plymouth Marine Laboratory (PML).

Methods.

Samples were collected from the underway seawater supply approximately every six hours. Before sampling, the sampling flask was rinsed three times with the seawater to be sampled. At the end of each day, the filtration equipment was rinsed with Milli-Q water. A volume of 100 mL was filtered using polycarbonate hydrophilic filters with pore sizes of 20 µm, 2 µm, and 0.1 µm. The filters were placed in 15mL centrifuge tubes. After filtration, the samples were stored in a freezer overnight. The following morning, 10.0 mL of 90% acetone was added to each sample, which was then returned to the freezer for an additional night. Before measurement, the samples were thawed for at least one hour. Subsequently, fluorometric measurements were performed, and the relative fluorescence unit (RFU) values were recorded in an Excel sheet to calculate the chlorophyll-a concentration (µg/L).

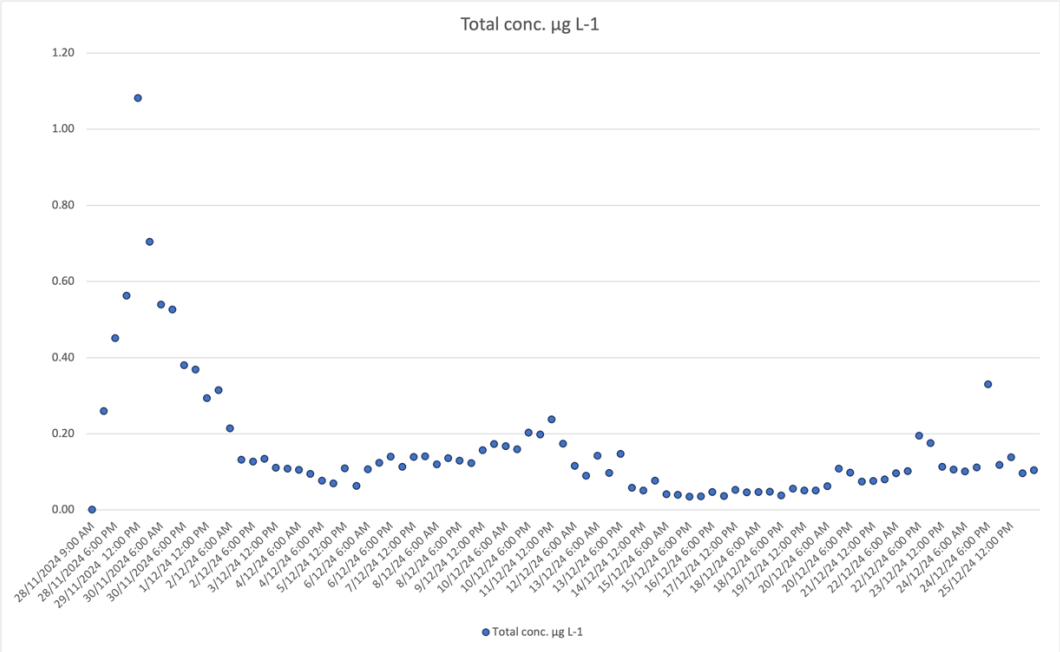

Figure 11. Total Chlorophyll-a concentration (µg/L) between 28/11/2024 09:00 AM until 25/12/2024 06:00 PM.

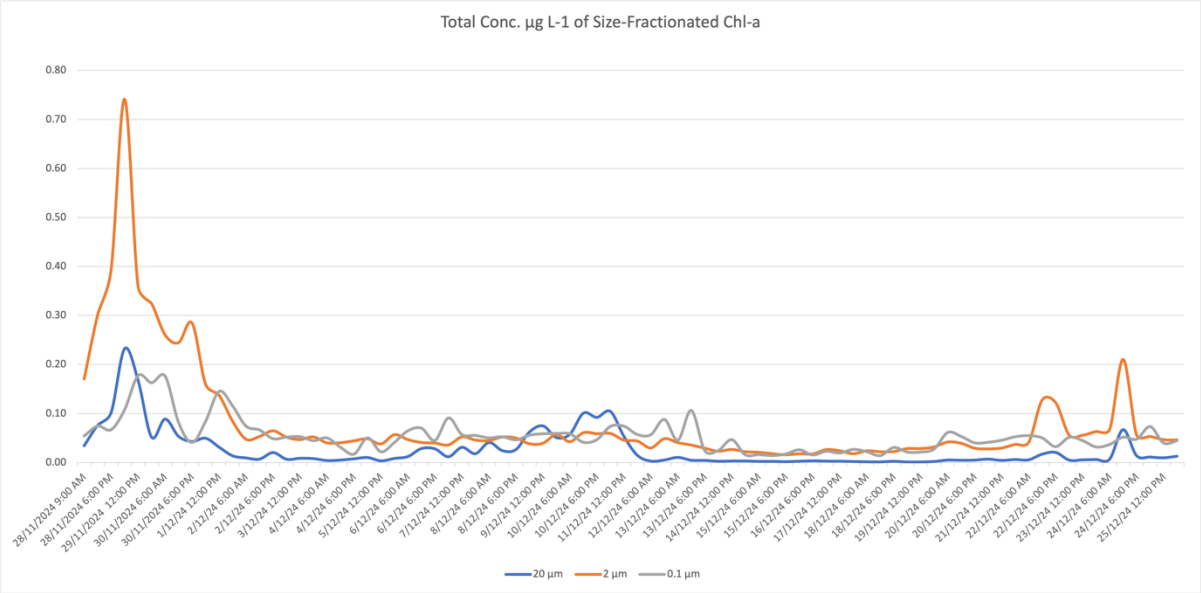

Figure 12. Total Chlorophyll-a concentration (µg/L) of Size-Fractionated (20µm, 2µm and 0.1µm) between 28/11/2024 09:00 AM until 25/12/2024 06:00 PM.

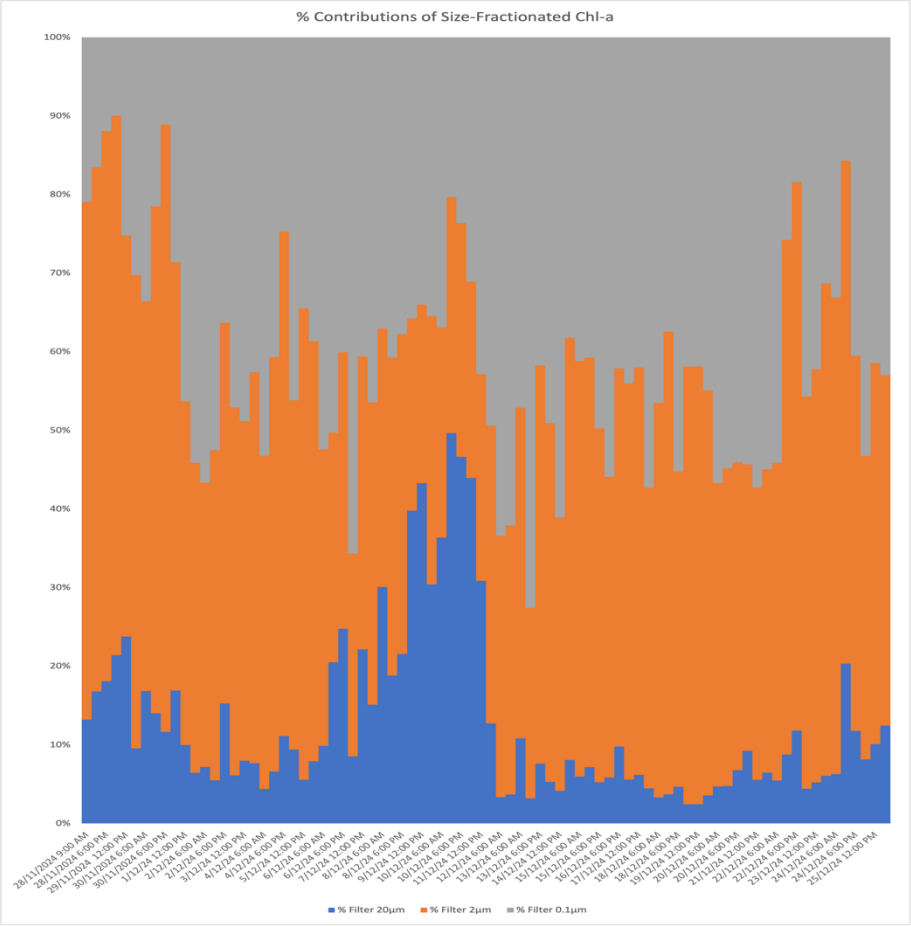

Figure 13. The contribution of Size-Fractionated (20µm, 2µm, and 0.1µm) for the total concentration (µg/L) between 28/11/2024 09:00 AM until 25/12/2024 06:00 PM.

Continuous single turn-over active fluorescence (LabSTAF).

Run by Gavin Tilstone and Francielle N. de. L Holtz Santos for:

Nina Schuback, Swiss Polar Institute, EPFL, Switzerland (schuback.nina@gmail.com);
Mark Moore, NOC, University of Southampton, UK, (c.moore@noc.soton.ac.uk);
Kevin Oxborough, Chelsea Technologies Ltd, UK, (koxborough@chelsea.co.uk).

Objective.

Continuous sampling of phytoplankton photo-physiology with a LabSTAF instrument connected to the underway water supply.

Method.

Two LabSTAF instruments were connected to the continuous seawater supply and automatically exchanged seawater samples to acquired fluorescence light curves (FLCs) at approximately 20 min intervals. The ratio of variable fluorescence detected at 685 nm and 730 nm, which has been developed as a proxy for pigment packaging (Boatman et al., 2019), was measured before each FLC. Furthermore, the measurement protocol included the automatic acquisition of variable fluorescence at 7 different excitation wavelengths to construct a photochemical excitation profile (PEP). This is used for real time spectral correction of FLC data. Two slightly different measurement protocols were run on the two instruments in order to assess the effect on derived parameters.

References.

Boatman, T. G., Geider, R. J. and Oxborough, K.: Improving the Accuracy of Single Turnover Active Fluorometry (STAF) for the Estimation of Phytoplankton Primary Productivity (PhytoPP), Front. Mar. Sci., 6, doi:10.3389/fmars.2019.00319, 2019

Discrete Hyperspectral Measurements of the optical properties of surface waters along a meridional transect in the Atlantic.

Peter Croot[1,2]

[1]*Earth and Ocean Sciences, School of Natural Sciences and Ryan Institute, University of Galway, Ireland;* [2]*Irish Centre for Research in Applied Geoscience (iCRAG), University of Galway, Ireland;*

Objectives/Goal

Despite much progress over the last two decades, there is still currently a lack of data worldwide for CDOM (Coloured dissolved organic matter) and FDOM (Fluorescent Dissolved Organic Matter) properties of the different oceanic regions (Nelson and Gauglitz, 2016; Nelson and Siegel, 2013; Röttgers and Doerffer, 2007). Particulate absorption is also a key control on the reflectance spectra observed by satellites (Jordan et al., 2024). As CDOM and particles contribute to the attenuation of light in seawater it has an impact on satellite retrievals for ocean colour and in particular the estimation of chlorophyll a in seawater. Automated continuous multispectral or hyperspectral sampling systems for CDOM and particulate absorption are helping to address this data gap (see section on this in this report) but there is still the need to acquire hyperspectral data from discrete sampling for comparison and for further developing the metrological aspects of this work.

There have been a number of earlier Atlantic meridional transects that have reported CDOM and/or FDOM data (Heller et al., 2013; Kowalczuk et al., 2013; Sabbaghzadeh et al., 2024) that this work builds upon. The recent publication of a compilation of particulate absorption data from earlier AMT (Jordan et al., 2024) has also helped guide the work here. The present work in AMT31, confined to surface waters only was to take measurements of CDOM & FDOM along the meridional transect to examine three main objectives/questions:

(i) To determine surface optical properties along the transect in support of satellite calibration/validation activities. To examine the relevant metrological aspects of discrete measurements of CDOM, FDOM and particulate absorption at sea with respect to accuracy and precision.

(ii) Examine whether protein or humic components can be identified in FDOM fluorescence from the Atlantic Gyres? To what extent is the water truly photo bleached?

(iii) What is the relationship between CDOM and *in situ* chlorophyll in oceanic gyres (Morel et al., 2010) ?

Methods

Samples from the ships non-toxic underway system were filtered (0.2 µm Sarstedt) and analysed for CDOM absorbance and fluorescence. CDOM absorbance was measured using a 1 m pathlength liquid waveguide capillary cell (LWCC-4100) coupled to an Ocean Optics MAYA spectrophotometer (Miller et al., 2002) and Ocean Optics DH-2000 BAL light source. All CDOM absorbance and fluorescence signals were normalized to ultrapure water supplied from the onboard Milli-Q IQ7010 system in the chemistry laboratory. Final CDOM data is corrected for

the effect of salinity (refractive index). Particulate absorption measurements were made onboard using two methods:

(i) by calculating the difference between direct measurement of unfiltered water with the same LWCC-4100 as used for CDOM and the filtered CDOM measurement.

(ii) using the quantitative filter method (QFT) (Mitchell and Kiefer, 1988) with GF/F filter and a QFT holder (WPI) connected to the same Ocean Optics spectrophotometer and light source used for the CDOM measurements.

FDOM fluorescence was measured by obtaining 3D Excitation Emission Matrix (EEM) spectra using an Aqualog (Horiba Scientific) fluorometer. EEMs are constructed from a matrix of measurements spanning a range of excitation and emission wavelengths. All spectra were corrected automatically for internal absorption and for Rayleigh and Raman scattering. Post processing of the data will be performed using PARAFAC (Parallel Factor Analysis) analysis via existing Matlab™ routines (Murphy et al., 2013; Stedmon and Bro, 2008).

References

Heller, M.I., Gaiero, D.M. and Croot, P.L., 2013. Basin scale survey of marine humic fluorescence in the Atlantic: Relationship to iron solubility and H_2O_2. Global Biogeochemical Cycles, 27(1): 88-100.

Jordan, T.M. et al., 2024. A compilation of surface inherent optical properties and phytoplankton pigment concentrations from the Atlantic Meridional Transect. Earth Syst. Sci. Data Discuss., 2024: 1-33.

Kowalczuk, P., Tilstone, G.H., Zabłocka, M., Röttgers, R. and Thomas, R., 2013. Composition of dissolved organic matter along an Atlantic Meridional Transect from fluorescence spectroscopy and Parallel Factor Analysis. Marine Chemistry, 157: 170-184.

Miller, R.L., Belz, M., Castillo, C.D. and Trzaska, R., 2002. Determining CDOM absorption spectra in diverse coastal environments using a multiple pathlength, liquid core waveguide system. Continental Shelf Research, 22(9): 1301-1310.

Mitchell, G.B. and Kiefer, D.A., 1988. Chlorophyll α specific absorption and fluorescence excitation spectra for light-limited phytoplankton. Deep Sea Research Part A. Oceanographic Research Papers, 35(5): 639-663.

Morel, A., Claustre, H. and Gentili, B., 2010. The most oligotrophic subtropical zones of the global ocean: similarities and differences in terms of chlorophyll and yellow substance. Biogeosciences, 7(10): 3139-3151.

Murphy, K.R., Stedmon, C.A., Graeber, D. and Bro, R., 2013. Fluorescence spectroscopy and multi-way techniques. PARAFAC. Analytical Methods, 5(23): 6557-6566.

Nelson, N.B. and Gauglitz, J.M., 2016. Optical Signatures of Dissolved Organic Matter Transformation in the Global Ocean. Frontiers in Marine Science, 2(118).

Nelson, N.B. and Siegel, D.A., 2013. The Global Distribution and Dynamics of Chromophoric Dissolved Organic Matter. Annual Review of Marine Science, 5(1): 447-476.

Röttgers, R. and Doerffer, R., 2007. Measurements of optical absorption by chromophoric dissolved organic matter using a point-source integrating-cavity absorption meter. Limnology And Oceanography-Methods, 5: 126-135.

Sabbaghzadeh, B., Uher, G. and Upstill-Goddard, R., 2024. Dynamics of chromophoric dissolved organic matter in the Atlantic Ocean: unravelling province-dependent relationships, optical complexity, and environmental influences. Frontiers in Marine Science, 11.

Stedmon, C. and Bro, R., 2008. Characterizing dissolved organic matter fluorescence with parallel factor analysis: a tutorial. Limnol. Oceanogr. Methods, 6: 572-579.

DNA sample collection.

Francielle N. de L. Holtz Santos, POGO Fellowship currently at AWI, Germany, (fr.holtz@gmail.com) *with Karen Tait, PML* (ktait@pml.ac.uk).

Cruise Objectives.

DNA materials of seawater samples were collected for Plymouth Marine Laboratory (PML) DNA archives.

Methods.

Samples from the underway seawater supply were taken every ~6 hrs. 5.0 L of seawater was collected into a sampling carboy. Sampling carboys were rinsed three times with sample water before sampling. Filtration tubes were rinsed with sample water before filtration. During the cruise, samples were collected for PML and for the University of South California. Seawater samples were filtered through Millipore Sterivex-GP, 0.22µm sterile vented filter units (SVGP01050) using a Cole-Palmer MasterFlex L/S Multichannel Pump (Model 7535-08). After filtration, samples were preserved by adding 1.0 mL of RNAlater Solution (Invitrogen by Thermo Fisher Scientific). Afterwards, all Sterivex units were sealed with tube sealing compound and Cole-Palmer Male Luer Lock plugs and stored at -80^{o}C in a freezer until return to PML for laboratory analysis.

Satellite Imagery.

Emma Sullivan, Will Jay, Dan Clewley, National Earth Observation Data Archive and Analysis Service (NEODAAS), PML, UK.

Satellite imagery were sent to the ship in near real time on a daily basis by NEODAAS, to inform the cruise of the salient surface sea surface temperature and phytoplankton chlorophyll *a* along the AMT31 track and to aid directing the ship when possible. The daily satellite images were predominantly from Sentinel-3 SLSTR and OCLI, though MUR SST and Suomi-VIIRS were also used when coverage from Sentinel-3 was limited. The images were processed for the area around the ships location and weekly composites were used to complement the daily images when coverage was poor due to cloud. A series of SST and Ocean Colour images that were sent out by NEODAAS from 24-11-2024 to 23-12-2024 are given in Figures 14 to 26, below.

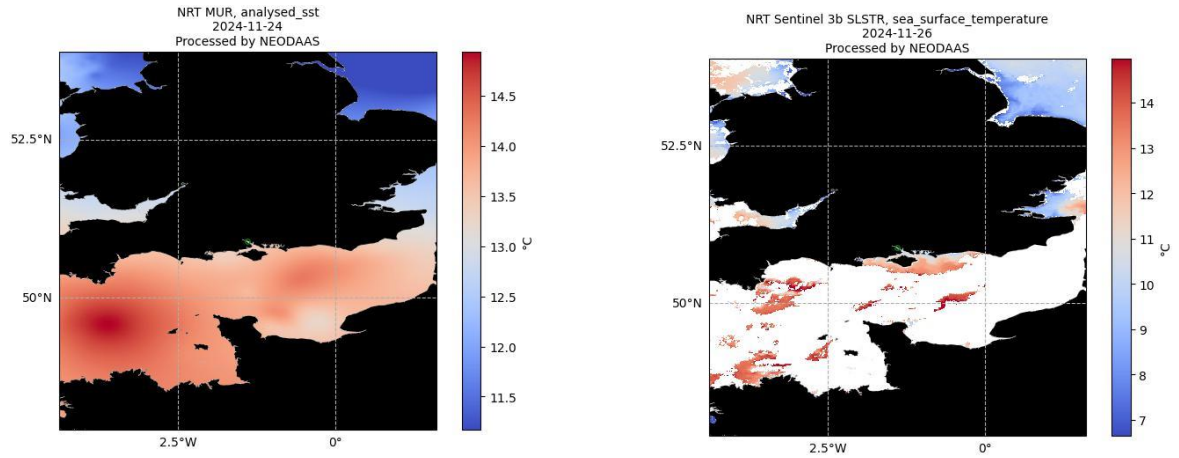

Figure 14. Near real time (NRT) Multi-scale Ultra-high Resolution (MUR) Sea surface temperature (SST) image of the English Channel from 24 November 2024 (left) and Sentinel 3b SST from 26 November 2024 (Right).

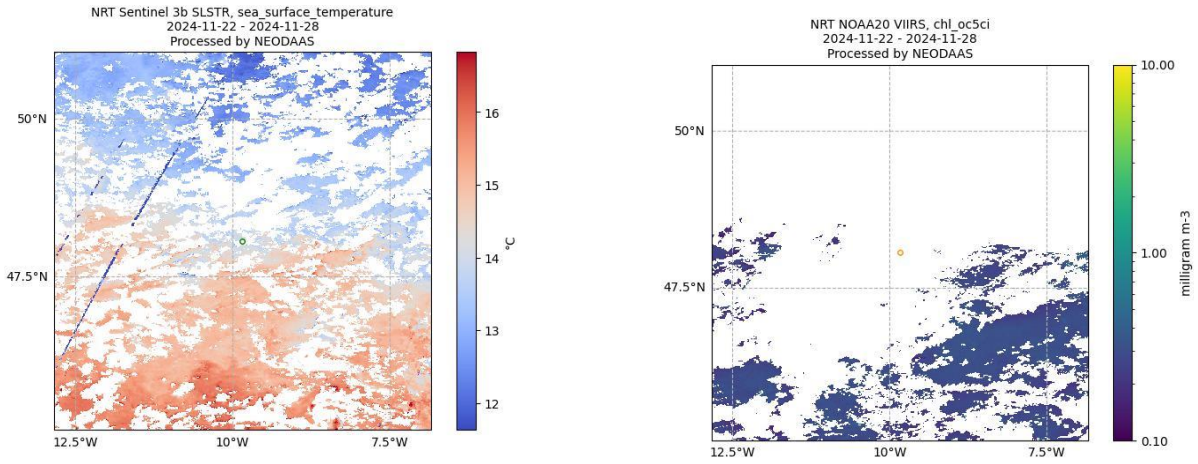

Figure 15. Near real time Sea surface temperature (SST) composite Sentinel 3b SST satellite image for the Celtic Sea shelf break and Bay of Biscay from 22 to 28 November 2024 (left) and NOAA20 VIIRS ocean colour Chlorophyll OC5CI product from 22 to 28 November 2024 (Right).

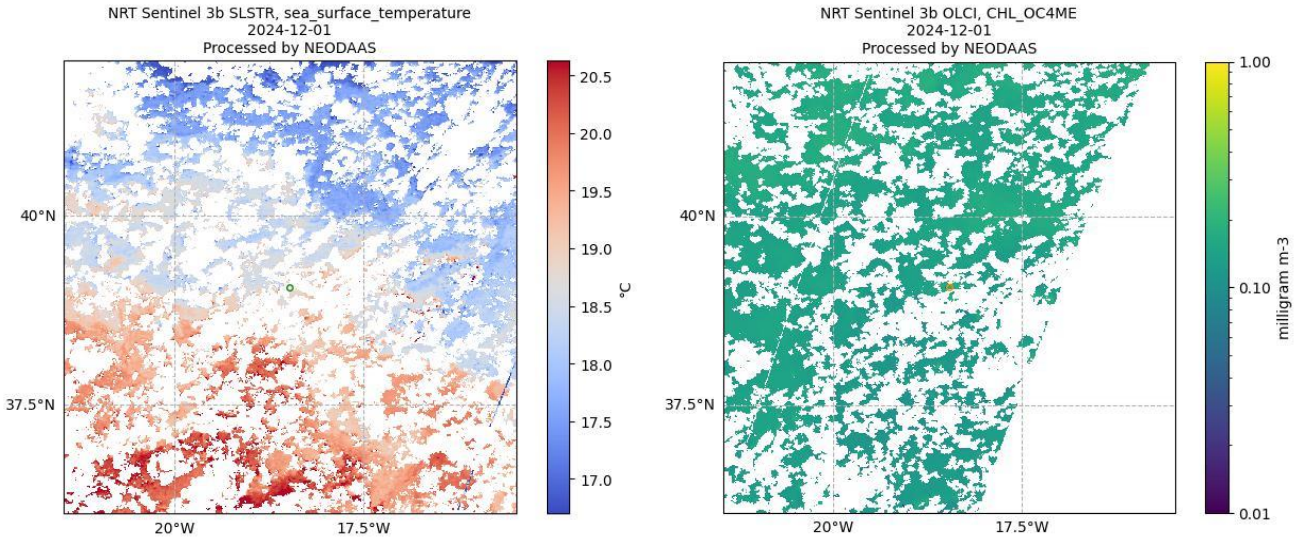

Figure 16. Near real time Sentinel 3b Sea surface temperature from SLSTR (left) and ocean colour from OLCI Chlorophyll OC4ME (right) images off Portugal from 01 December 2024.

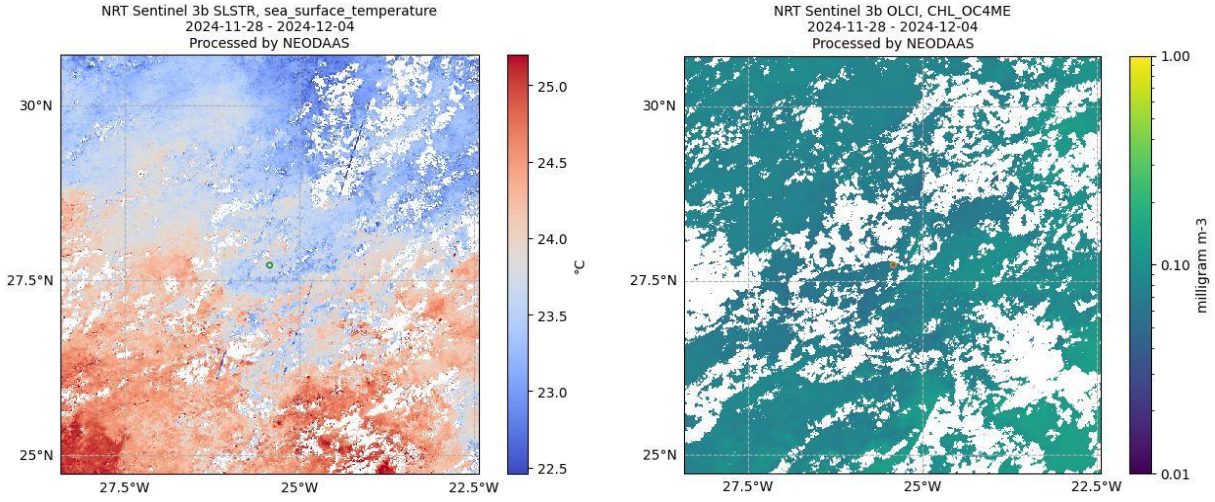

Figure 17. Near real time Sentinel 3b Sea surface temperature from SLSTR (left) and ocean colour from OLCI Chlorophyll OC4ME (right) composite images from 28 November to 04 December 2024 off Morrocco.

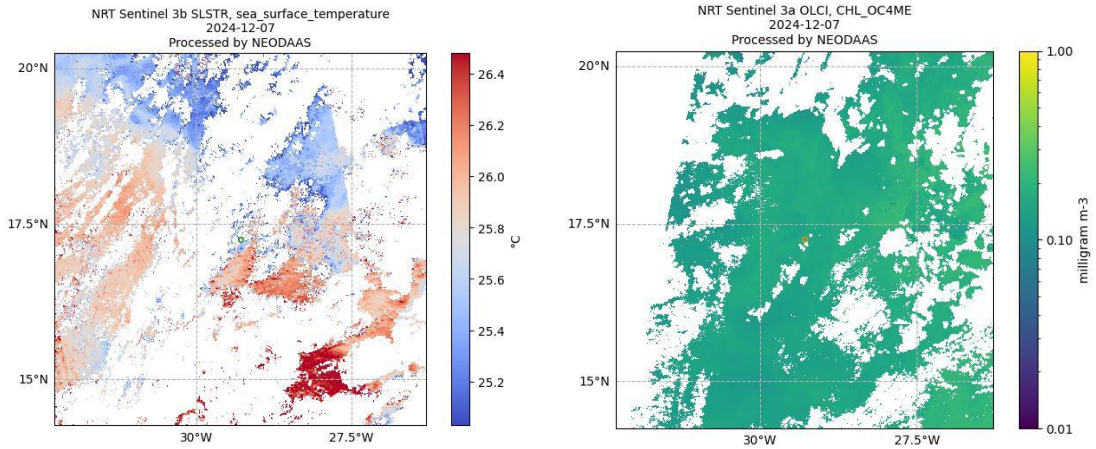

Figure 18. Near real time Sentinel 3b Sea surface temperature from SLSTR (left) and ocean colour from OLCI Chlorophyll OC4ME (right) images from 07 December 2024 near to the Canary Islands.

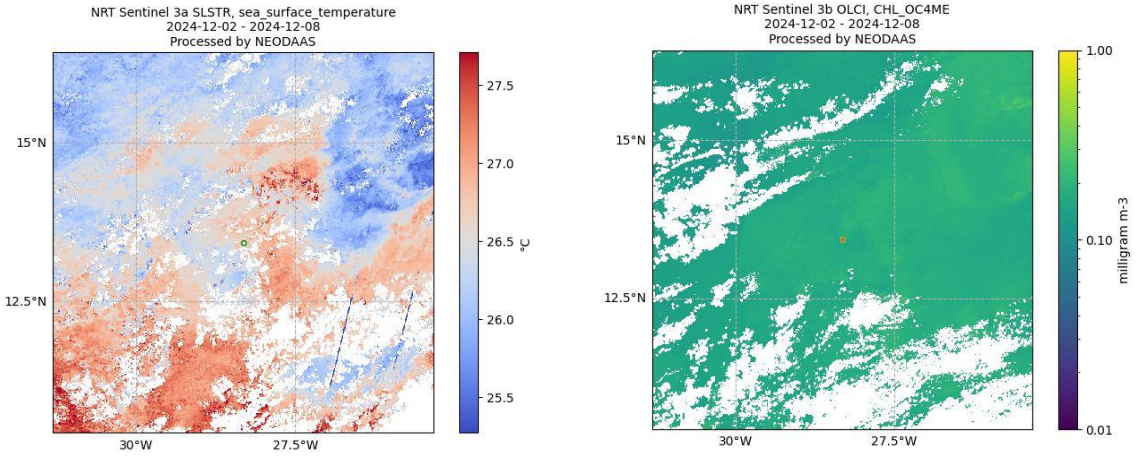

Figure 19. Near real time Sea surface temperature (SST) composite Sentinel 3b SST satellite image off Cape Verde from 02 to 08 December 2024 (left) and Sentinel 3b OLCI ocean colour Chlorophyll OC4ME product from 02 to 08 December 2024 (Right).

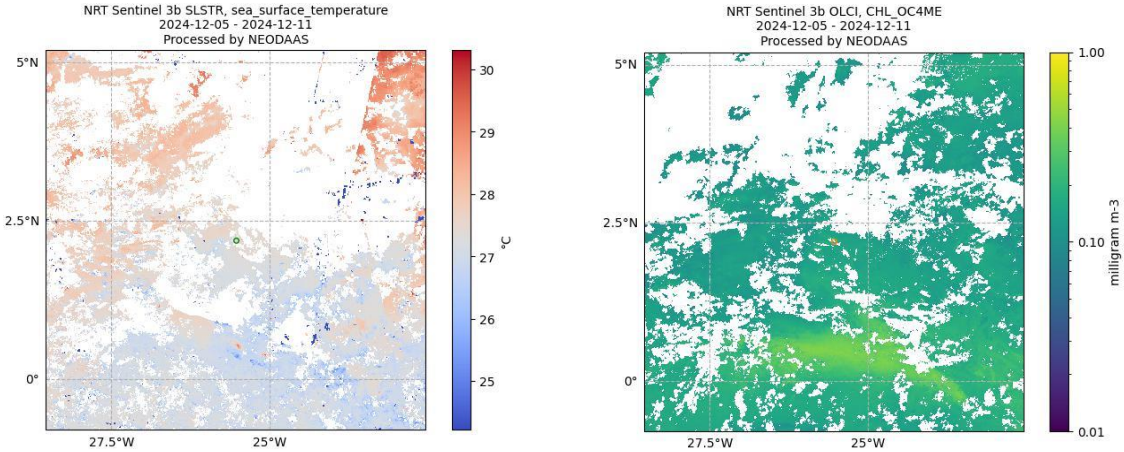

Figure 20. Near real time Sea surface temperature (SST) composite Sentinel 3b SST satellite image north of the Equator from 05 to 11 December 2024 (left) and Sentinel 3b OLCI ocean colour Chlorophyll OC4ME product from 05 to 11 December 2024 (Right).

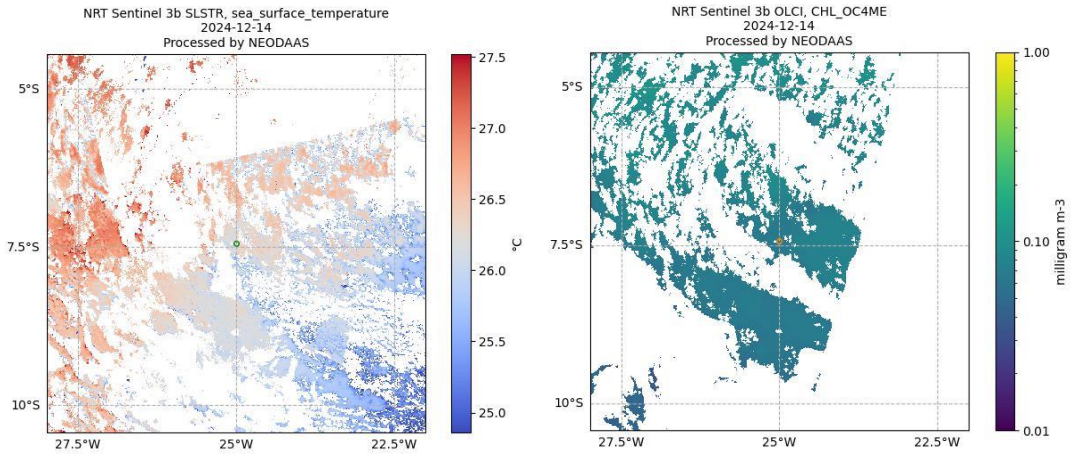

Figure 21. Near real time Sea surface temperature (SST) composite Sentinel 3b SST satellite image south of the Equator from 14 December 2024 (left) and Sentinel 3b OLCI ocean colour Chlorophyll OC4ME product (Right).

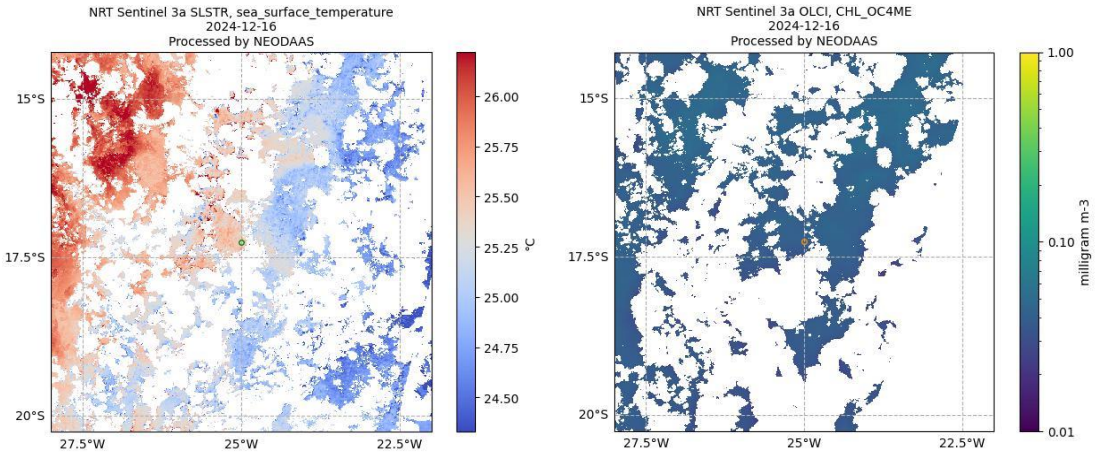

Figure 22. Near real time Sea surface temperature (SST) composite Sentinel 3b SST satellite image south of the Equator from 16 December 2024 (left) and Sentinel 3b OLCI ocean colour Chlorophyll OC4ME product (Right).

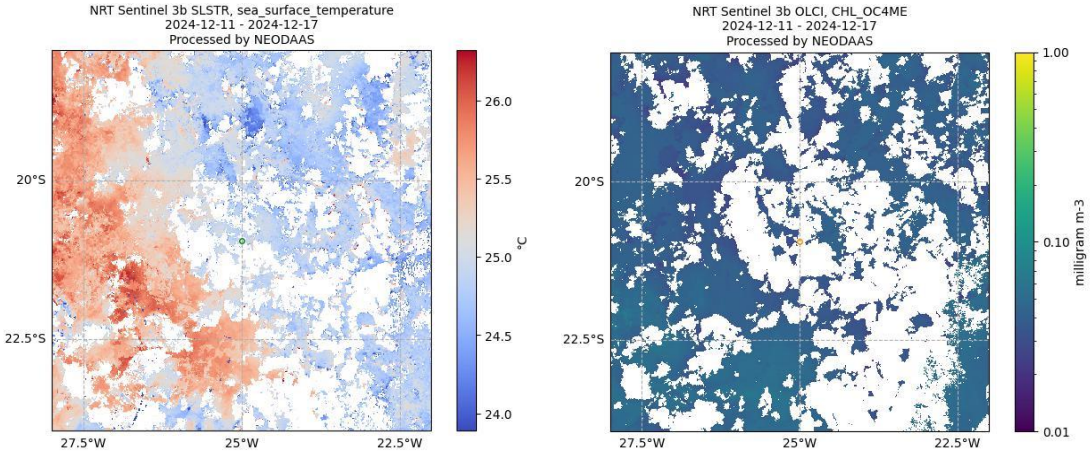

Figure 23. Near real time Sea surface temperature (SST) composite Sentinel 3b SST satellite image south of the Equator from 11 to 17 December 2024 (left) and Sentinel 3b OLCI ocean colour Chlorophyll OC4ME product (Right).

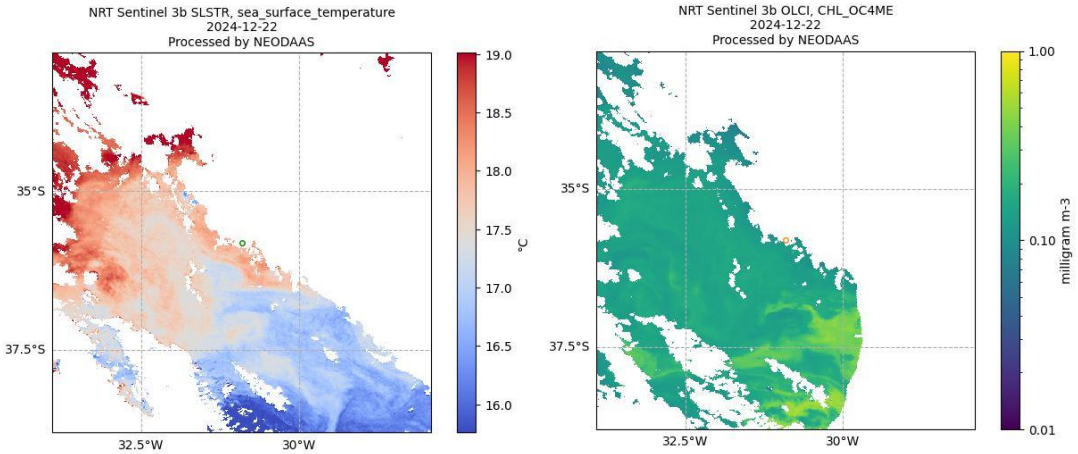

Figure 24. Near real time Sea surface temperature (SST) Sentinel 3b SLSTR satellite image between 34 and 38 °S from 22 December 2024 (left) and Sentinel 3b OLCI ocean colour

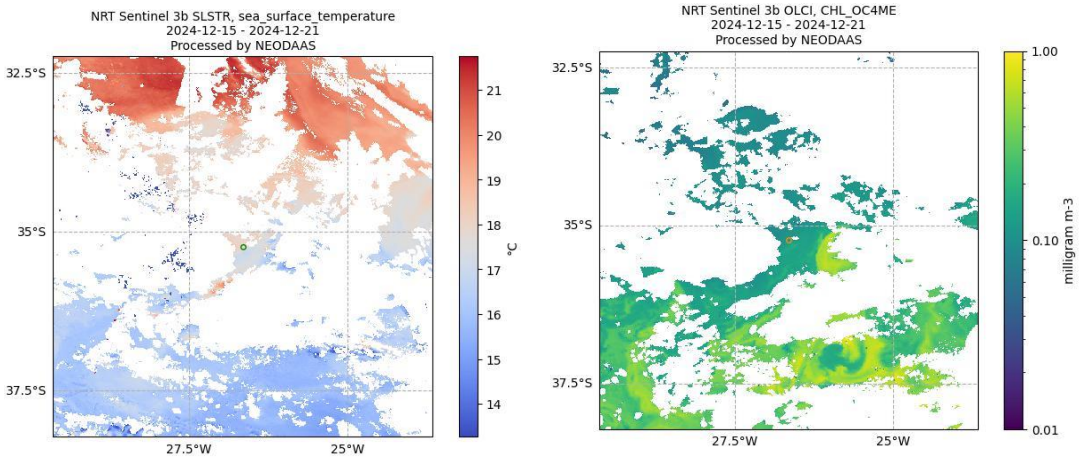

Figure 25. Near real time Sea surface temperature (SST) Sentinel 3b SLSTR satellite composite image between 32.5 and 37.5 °S from 15 to 21 December 2024 (left) and Sentinel 3b OLCI ocean colour Chlorophyll OC4ME product (Right).

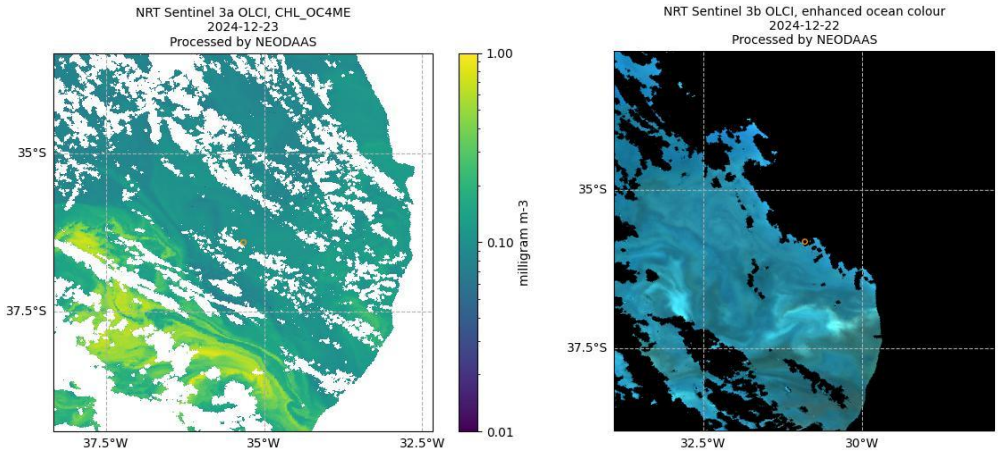

Figure 26. Near real time Sentinel 3b OLCI ocean colour Chlorophyll OC4ME product satellite image between 34 and 38 °S from 23 December 2024 (left) and Sentinel 3b OLCI enhanced ocean colour from 22 December 2024 (Right).

NMF Scientific Ship Systems.

Mark Maltby, (anmo@noc.ac.uk) Scientific Ship Systems, NMF, National Oceanography Centre

Ship Scientific Systems (SSS) is responsible for operating and managing the Ship's scientific information technology infrastructure, data acquisition, compilation and delivery, and the suite of ship-fitted instruments and sensors in support of the Marine Facilities Programme (MFP)

The work site was the eastern OSNAP array across the Rockall Plateau.

The main objectives for SSS in the service of the science party on this cruise were:

1. Acquire underway data and metadata, including sea-surface, meteorological, position and attitude, depth.
2. Provide services for recording metadata and events and monitoring data streams.
3. Provide basic IT support.

All times in this report are in UTC.

Scientific computer systems

Underway data acquisition

Data from the suite of ship-fitted scientific instrumentation was aggregated onto a network drive on the ship's file server. This was available throughout the voyage in read-only mode to permit

scientists to work with the data as it was acquired. A Public network folder was also available for scientists to share files.

A copy of these two drives are written to the end-of-cruise disks that are provided to the Principal Scientist and the designated data centre.

The designated data centre for this cruise is: British Oceanographic Data Centre

---

List of logged ship-fitted scientific systems:

`/Cruise_Reports/[Keywords]_Ship_fitted_information_sheet.docx`

The data acquisition systems used on this cruise are detailed in the table below. The data and data description documents are filed per system in the *Data* and *Documentation* directories respectively within Ship Systems folder on the cruise data disk.

Table 1: Data acquisition systems used on this cruise.

Data acquisition system	Usage	Data products	Directory system name
Ifremer TechSAS	Continuous	NetCDF ASCII pseudo-NMEA	`/TechSAS/`
NMF RVDAS	Continuous	ASCII Raw NMEA	`/RVDAS/`
Kongsberg SIS (EM122)	Discrete	Kongsberg .all	`/Acoustics/EM-122/`
Kongsberg SIS (EM710)	Discrete	Kongsberg .all	`/Acoustics/EM-710/`
Kongsberg EA640	Continuous	None, redirected to Techsas/RVDAS RAM	`/Acoustics/EA-640/`
UHDAS (ADCPs)	Continuous	ASCII raw, RBIN, GBIN, CODAS files	`/Acoustics/ADCP/`

Data description documents per system:

/Ship_Systems/Documentation/[systemName]/

Data directories per system:

/Ship_Systems/Data/[systemName]/

Significant acquisition events and gaps

On this cruise, the NMF Event Logger was used with CSV records of events saved to the cruise data directory.

Path and pattern to event log CSV files:

/Cruise_Reports/Event_Logs/[logtype]/[logName]/*.csv

From the 28th to the 11th the timestamp on the Techsas and RVDAS data loggers was experiencing irregularities due to a NTP clock synchronisation issue. This was resolved after the 11/12/24. The RVDAS files can't be corrected as the OS gradually amended the time back. In the Techsas files there is a circa 30 secs jump forward and then some hours later a circa 30 secs jump back. The Techsas NMEA ascii files have been corrected. Below shows the time jumps as per the PosMV GPS files.

Date	Jump Forward	Jump Backward	Jump delta
28/11/24	01:00:08	03.:26:22	32.2 s
29/11/24	01:00:15	03:52:40	31.4 s
30/11/24	01:00:36	03:25:56	31.5 s
01/12/24	01:00:09	03:45:43	31.6 s
02/12/24	01:00:32	03:49:15	31.8 s
03/12/24	01:00:18	03:30:43	32.9 s
04/12/24	01:00:14	03:41:23	33.1 s
05/12/24	01:00:13	02:48:49	32.2 s
06/12/24	01:00:16	03:30:19	32.3 s

07/12/24	01:00:25	03:30:53	32.4 s
08/12/24	01:00:27	03:31:37	32.5 s
09/12/24	01:00:14	03:48:35	32.6 s
10/12/24	01:00:09	03:34:11	32.7 s
11/12/24	01:00:19	01:10:12	33.8 s
11/12/24	01:58:22	02:28:23	32.8 s

There was a gap in the Surfmet data due to a flood in the met lab cutting power from 18/12/24 21:56:05 – 19/12/24 12:03:22 - 14hr 7min 17s downtime

Internet provision

Satellite communications were provided with Starlink, VSat and Iridium Certus.

*Note: OneWeb should have been the main high-speed internet link instead of Starlink, but it is still not fully operational.

The ship operated with bandwidth controls to prioritise business use.

Outreach and streaming

Social Media posts

Instrumentation

Coordinate reference

Path to ship survey files:

`/Ship_Systems/Documentation/Vessel_Survey`

Origin (RRS James Cook)

The common coordinate reference was defined by the Blom Maritime survey (2006) as:

1. The reference plane is parallel with the main deck abeam (transversely) and with the baseline (keel) fore- and aft-ways (longitudinally).
2. Datum (X = 0, Y = 0, Z = 0) is centre topside of the Applanix motion reference unit (MRU) chassis.

Multibeam

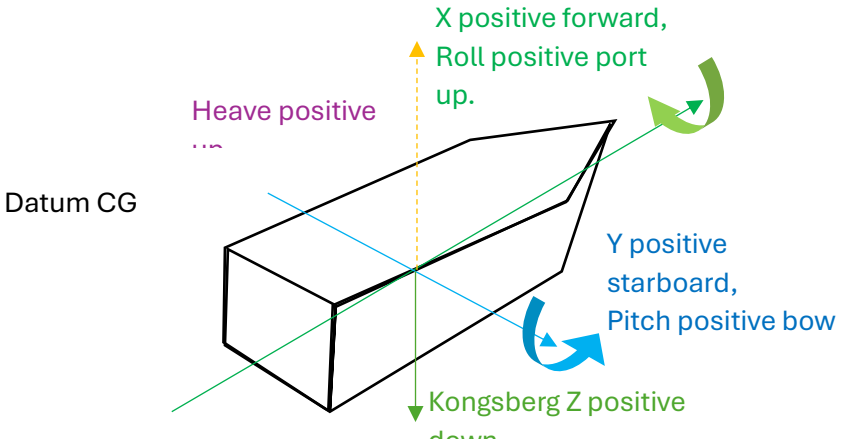

Figure 1: Conventions used for position and attitude. On the Discovery, the Datum is the CRP at the CG. On the Cook the Datum is on the centre, topside of the Applanix MRU.

The Kongsberg axes reference conventions are (see Figure 1) as follows:

1. X positive forward,
2. Y positive starboard,
3. Z positive downward.

The rotational sense for the multibeam systems and Seapath is set to follow the convention of Applanix PosMV (the primary scientific position and attitude system), as per Figure 1.

Primary scientific position and attitude system

The translations and rotations provided by this system (Applanix PosMV) have the following convention:

1. Roll positive port up,
2. Pitch positive bow up,
3. Heading true positive to starboard,
4. Heave positive up.

Position, attitude and time

System	Navigation (Position, attitude, time)

Data product(s)	NMEA (mvpos,mvatt,spatt,sppos,cnpos):
	`/Ship_Systems/Data/TechSAS/NMEA/`
	NetCDF (GPS): `/Ship_Systems/Data/TechSAS/NetCDF/`
	Raw NMEA (POSMV,SEAPATH,CNAV):
	`/Ship_Systems/Data/RVDAS/rawdata`

Data description	`/Ship_Systems/Documentation/GPS_and_Attitude/Data_Description`
Other documentation	`/Ship_Systems/Documentation/GPS_and_Attitude`

Component	Purpose	Outputs	Headline Specifications
Applanix PosMV	Primary GPS and attitude.	Serial NMEA to acquisition systems and multibeam	Positional accuracy within 0.15 m.
Kongsberg Seapath 330	Secondary GPS and attitude.	Serial and UDP NMEA to acquisition systems and multibeam	Positional accuracy within 1 m.
Oceaneering CNav 3050	Correction service for primary and secondary GPS and dynamic positioning.	RTCM to primary and secondary GPS	Positional accuracy within 0.15 m.
Meinberg NTP Clock	Provide network time	NTP protocol over the local network.	

Ocean and atmosphere monitoring systems

SURFMET

System	SURFMET (Surface water and atmospheric monitoring)	

Data product(s)	NMEA (surfm,sbe38,sbe45,winds):
	`/Ship_Systems/Data/TechSAS/NMEA/`
	NetCDF (SURFMETV3, SBE38,TSG,WINDSONIC):
	`/Ship_Systems/Data/TechSAS/NetCDF/`
	Raw NMEA (SURFMET,SBE38,SBE49, WINDSONIC):
	`/Ship_Systems/Data/RVDAS/rawdata`	

Data description	`/Ship_Systems/Documentation/Surfmet/Data_Description`	
Other documentation	`/Ship_Systems/Documentation/Surfmet`	
Calibration info	See Ship Fitted Sensor sheet for calibration info for each sensor & calibration files. `/Ship_Systems/Documentation/Surfmet/Calibration_Files`	
Component	**Purpose**	**Outputs**
Inlet temperature probe (SBE38)	Measure temperature of water at hull inlet.	Serial to Interface Box.
Drop keel temperature probe (SBE38)	Measure temperature of water in drop keel space.	Serial to Interface Box.
Thermosalinograph (SBE45)	Measure temp. and conductivity at sampling board. Salinity is calculated.	Serial to Interface Box.
Interface Box (SBE90402)	Signals management.	Serial to Moxa.
Debubbler	Reduces bubbles through instruments.	None.
Transmissometer (CST)	Measure of transmittance.	Analogue to NUDAM.

Fluorometer (WS3S)	Measure of fluorescence.	Analogue to NUDAM.
Air temperature and humidity probe (HMP45A, HMP155)	Temperature and humidity at met. platform.	Analogue to NUDAM.
Ambient light sensors (PAR, SKE510; TIR, CMP6)	Ambient light at met. platform.	Analogue to NUDAM.
Barometer (PTB110, PTB210)	Atmospheric pressure at met. platform.	Analogue to NUDAM.
Anemometer (Windsonic)	Wind speed and direction at met. platform.	Serial to Moxa.
NUDAM	A/D converter.	Serial NMEA to Moxa.
Moxa	Serial to UDP converter.	UDP NMEA to Surfmet VM.
Surfmet Virtual Machine	Data management.	UDP NMEA to TechSAS, RVDAS.

Component	Calibrated product steps
SBE38: Temperature (°C)	No calibration to apply because the residuals are below uncertainty.
SBE45: Temperature (°C)	No calibration to apply because the residuals are below uncertainty.
SBE45: Conductivity (S m^{-1})	No calibration to apply because the residuals are below uncertainty.
CST: Transmission (%)	$\text{Product} = (\text{Data} - V_{\text{dark}})/(V_{\text{ref}} - V_{\text{dark}})$. Here product has units % and data, V_{dark} and V_{ref} have units V.
WS3S: Fluorescence (µg L^{-1})	$\text{Product} = \text{Coefficient} \times (\text{Data} - \text{Offset})$. Here product has units µg L^{-1}, coefficient has units µg L^{-1} V^{-1}, and data and offset have units V.

HMP155: Temperature (°C)	No calibration to apply because the residuals are below uncertainty.
HMP45A / HMP155: Relative humidity (%)	No calibration to apply because the residuals are below uncertainty.
PTB110: Pressure (hPa)	No calibration to apply because the residuals are below uncertainty.
SKE510: PAR (W m^{-2})	$\text{Product} = \text{Data} \times \left(\frac{10^6}{\text{Coefficient}}\right)$. Here product has units W m^2, data has units 10^{-5} V, the 10^6 scalar has units μV V^{-1}, and coefficient has units μV m^2 W^{-1}.
CMP6: TIR (W m^{-2})	$\text{Product} = \text{Data} \times \left(\frac{10^6}{\text{Coefficient}}\right)$. Here product has units W m^2, data has units 10^{-5} V, the 10^6 scalar has units μV V^{-1}, and coefficient has units μV m^2 W^{-1}.
Windsonic: Wind speed (m s^{-1})	No calibration to apply.
Windsonic: Wind direction (m s^{-1})	No calibration to apply.

Note that while the residuals (difference of reference and measured) are below uncertainty and the output is considered calibrated for the SBE38, SBE45, HMP45A, HMP155, PTB110 and PTB210 instruments, a regression could still be made between the reference and measured data (see the calibration certificate) if desired. Follow the steps below:

1. Calculate $y = Bx + A$ from calibration data, where x is reference data.
2. $\text{Product} = (\text{Data} - A)/B$.

The NMF Surfmet system was run throughout the cruise, excepting times for cleaning, entering and leaving port, and whilst alongside. Please see the separate information sheet for details of the sensors used and whether their recorded data have calibrations applied or not.

Surface water sampling board maintenance

Path to event log CSV files:

`/Cruise_Reports/Event_Logs/techlogs/SURFMET.csv`

The system was cleaned prior to the cruise.

Water samples taken 4 times a day for SBE45 comparison. Samples logged in event log.

Path to water sample event log CSV files:

`/Cruise_Reports/Event_Logs/scilogs/TSG_samples.csv`

Path to samples Autosal files:

/Ship_Systems/Documentation/Surfmet/TSG/

Wave radar

System	WAMOS Wave Radar	
Data product(s)	NMEA (wamos, rexwr): `/Ship_Systems/Data/TechSAS/NMEA/` NetCDF (NC): `/Ship_Systems/Data/TechSAS/NetCDF/` Raw NMEA (WAMOS, REX2): `/Ship_Systems/Data/RVDAS/rawdata`	
Data description	`/Ship_Systems/Documentation/Wamos/Data_Description`	
Other documentation	`/Ship_Systems/Documentation/Wamos`	
Component	Purpose	Outputs
Rutter OceanWaves WAMOS	Measure wave height, direction, period and spectra.	Summary statistics in NMEA to TechSAS and RVDAS. Spectra files.
RsAqua Rex2 Wave Height Sensor	Measure wave height at bow to provide calibration reference dataset.	Wave height NMEA, UDP to TechSAS, RVDAS.

The wave radar magnetron requires annual replacement. Following replacement, WAMOS needs to collect wave data within 5 km of another wave height sensor over the full range of sea-states in order to derive wave height calibration coefficients for the new magnetron. This reference dataset can be derived by examining the ship's track for wave buoys and downloading their data, or by using the onboard RsAqua Wave Height sensor fitted on the ship's bow.

Hydroacoustic Systems

System	Acoustics	

Data product(s)	Raw (EA-640, EM-122):
	`/Ship_Systems/Data/Acoustics`
	NMEA (eadep, emdep):
	`/Ship_Systems/Data/TechSAS/NMEA`
	NetCDF (EA600, DEPTH):
	`/Ship_Systems/Data/TechSAS/NetCDF`
	Raw NMEA (EA640, EM122cb):
	`/Ship_Systems/Data/RVDAS/rawdata`	

Data description	`/Ship_Systems/Documentation/Acoustics`	
Other documentation	`/Ship_Systems/Documentation/Acoustics`	
Component	Purpose	Operation and Outputs
10/12 kHz Single beam (Kongsberg EA-640)	Primary depth sounder	Continuous running NMEA over serial, raw files
12 kHz Multibeam (Kongsberg EM-122)	Full-ocean-depth multibeam swath.	Discrete Binary swath, centre-beam NMEA, *.all files, optional water column data
70 kHz Multibeam (Kongsberg EM-710)	Coastal/shallow multibeam swath.	Discrete Binary swath, *.all files.
Drop keel sound velocity sensor	Provide sound velocity at transducer depth	Continuous running Value over serial to Kongsberg SIS.
75 kHz ADCP (Teledyne OS75)	Along-track ocean current profiler	Continuous, free running (via UHDAS)
150 kHz ADCP (Teledyne OS150)	Along-track ocean current profiler	Continuous, free running (via UHDAS)
CARIS	Post-processing	Discrete CARIS Project file. CARIS Vessel files

Sound velocity profiles

Sound velocity profiles were calculated from the ISAS model using Ifremer DORIS.

Path of sound velocity profile data on the cruise datastore:

`/Ship_Systems/Data/Acoustics/Sound_Velocity`

Details of when sound velocity profiles were taken and applied in the eventlog

Path to event log CSV files:

`/Cruise_Reports/Event_Logs/techlogs/Swath_acoustics.csv`

Equipment-specific comments

ADCPs

Path of ADCP data on the cruise datastore:

`/Ship_Systems/Data/Acoustics/ADCP`

Attribute	Value
Acquisition software	UHDAS
Frequencies used	75 kHz, 150 kHz
Running mode	Free-running (untriggered)

Path of Multibeam data on the cruise datastore:

`/Ship_Systems/Data/Acoustics/EM-122`

Path of EM122 CARIS Vessel Configuration File:

`/Ship_Systems/Data/Acoustics/CARIS_Processed/VesselConfig`

<table>
<tr><th>Attribute</th><th>Value</th></tr>
<tr><td>Number of surveys</td><td>1, run in UK waters post EM710 run and in International waters.</td></tr>
<tr><td>Date of patch test</td><td>Not undertaken.</td></tr>
<tr><td>Offsets and rotations</td><td>
<table>
<tr><th>Item</th><th>X (m, + Forward)</th><th>Y (m, + Starboard)</th><th>Z (m, + Down)</th></tr>
<tr><td>Tx transducer</td><td>19.205</td><td>1.830</td><td>6.934</td></tr>
<tr><td>Rx transducer</td><td>14.094</td><td>0.950</td><td>6.932</td></tr>
<tr><td>Attitude 1</td><td>0</td><td>0</td><td>0</td></tr>
<tr><td>Attitude 2</td><td>-0.350</td><td>0.056</td><td>-0.373</td></tr>
<tr><td>Waterline</td><td></td><td></td><td>1.2</td></tr>
</table>
<table>
<tr><th>Item</th><th>Roll (deg)</th><th>Pitch (deg)</th><th>Yaw (deg)</th></tr>
<tr><td>Tx transducer</td><td>-0.35</td><td>-0.1</td><td>0.19</td></tr>
<tr><td>Rx transducer</td><td>-0.06</td><td>0.1</td><td>0.15</td></tr>
<tr><td>Attitude 1</td><td>0.15</td><td>0.12</td><td>-0.2</td></tr>
<tr><td>Attitude 2</td><td>0.06</td><td>0.16</td><td>0.03</td></tr>
</table>
</td></tr>
<tr><td>Post-processing undertaken</td><td>Caris project JC272</td></tr>
</table>

Path of Multibeam data on the cruise datastore:

`/Ship_Systems/Data/Acoustics/EM-710`

Path of EM710 CARIS Vessel Configuration File:

`/Ship_Systems/Data/Acoustics/CARIS_Processed/VesselConfig`

<table>
<tr><th>Attribute</th><th>Value</th></tr>
<tr><td>Number of surveys</td><td>1, on departure in UK shallow waters.</td></tr>
<tr><td>Date of patch test</td><td>Not undertaken.</td></tr>
<tr><td>Offsets and rotations

Tx Orient: Port
Rx Orient: Forward</td><td>
<table>
<tr><th>Item</th><th>X (m, + Forward)</th><th>Y (m, + Starboard)</th><th>Z (m, + Down)</th></tr>
<tr><td>Tx transducer</td><td>5.415</td><td>-0.015</td><td>6.965</td></tr>
<tr><td>Rx transducer</td><td>4.944</td><td>0.013</td><td>6.695</td></tr>
<tr><td>Attitude 1</td><td>0</td><td>0</td><td>0</td></tr>
<tr><td>Attitude 2</td><td>-0.350</td><td>0.056</td><td>-0.737</td></tr>
<tr><td>Waterline</td><td></td><td></td><td>1.2</td></tr>
</table>
<table>
<tr><th>Item</th><th>Roll (deg)</th><th>Pitch (deg)</th><th>Yaw (deg)</th></tr>
<tr><td>Tx transducer</td><td>-0.418</td><td>0.228</td><td>0</td></tr>
<tr><td>Rx transducer</td><td>0.130</td><td>0</td><td>0</td></tr>
<tr><td>Attitude 1</td><td>-0.45</td><td>0.68</td><td>-0.38</td></tr>
<tr><td>Attitude 2</td><td>-0.46</td><td>0.39</td><td>-1.01</td></tr>
</table>
</td></tr>
</table>

Post-processing undertaken	Caris project JC272

CARIS Project

System	Marine Gravimeter
Data product(s)	GeoTiff for each surface XYZ ascii for each surface
Surfaces	JC272_Cube_Auto_EM710 JC272_Cube_Auto_EM122
Cleaning	JC272_Cube_Auto_EM710 – Full line cleaning, no surface cleaning JC272_Cube_Auto_EM122 – Line cleaning in bad weather sections, no surface cleaning

Geophysics systems

Gravimeters

System	Marine Gravimeter		
Data product(s)	NMEA ( ): `/Ship_Systems/Data/TechSAS/NMEA` NetCDF (GRAV): `/Ship_Systems/Data/TechSAS/NetCDF` Raw NMEA ( ): `/Ship_Systems/Data/RVDAS/rawfiles` DgS Data Files: `/Ship_Systems/Data/Gravity`		
Data description	`/Ship_Systems/Documentation/Gravity/Data_Description`		
Other documentation	`/Ship_Systems/Documentation/Gravity`		
Component	Purpose	Outputs	Headline Specifications
DgS AT1M-12U Marine Gravimeter	Measure relative gravity while underway	Serial NMEA to acquisition systems and multibeam	Drift: Accuracy:

		Meter data files.	Resolution: Feature resolution:
L&R Land Gravimeter	Measure relative gravity between base station and quayside	Manual tie-in logsheets, tie-in spreadsheet.	

Gravimeter configuration and surveys

Attribute	Value				
Tie-in information	Tie-in	1	2	3	4
	Date	21/11/24			
	Port	GBSOU			
	Calculated absolute value (mGals)	98115.1957			
	Marine GM value (mGals)	12179.2			

Appendix 1 – Underway Sampling Log.

Table 3. Underway Sampling log for PML, Uni of Connecticut (UC) , Uni of Galway (UG) on AMT31.

						PML	PML	PML	PML	PML	PML	UC	UG	UG	UG
DATE	TIME (UTC)	TIME (SHIP)	LAT	LONG	SAMPLE ID	TA/DIC	AFC	pH	Nutrients	Chl-a (0.2, 2, 20 micron)	eDNA	LISST	aCDOM	fDOM	aph
28-Nov-2024	06:00	06:00	-4.1961	49.9104	UW001										
28-Nov-2024	09:00	09:00	-5.0226	49.7089	UW002		X			x					
28-Nov-2024	12:00	12:00	-5.7312	49.5128	UW003	X	X	X	X	x	x				
28-Nov-2024	15:00	15:00	-6.3533	49.2643	UW004	X	X	X	X						
28-Nov-2024	18:00	18:00	-6.9986	49.0563	UW005	X	X	X	X	x	x				
29-Nov-2024	06:00	06:00	-9.396	48.2714	UW006	X	X	X	X	x	x				
29-Nov-2024	09:00	09:00	-9.9056	48.0179	UW007	X	X	X	X			x			
29-Nov-2024	12:00	12:00	-10.3426	47.7382	UW008	X	X	X	X	x	x	x			
29-Nov-2024	15:00	15:00	-10.8177	47.427	UW009	X	X	X	X			x			
29-Nov-2024	18:00	18:00	-11.2568	47.1436	UW010	X	X	X	X	x	x	x			
30-Nov-2024	06:00	06:00	-13.0201	45.9705	UW011	X	X	X	X	x	x				
30-Nov-2024	09:00	09:00	-13.4802	45.6632	UW012	X	X	X	X			x			
30-Nov-2024	12:00	12:00	-13.8775	45.3936	UW013	X	X	X	X	x	x	x			
30-Nov-2024	15:00	15:00	-14.3287	45.09	UW014	X	X	X	X			x			
30-Nov-2024	18:00	18:00	-14.638	44.7261	UW015	X	X	X	X	x	x	x			
01-Dec-24	06:00	06:00	-15.9185	42.8896	UW016	X	X	X	X	x	x		x	x	x
01-Dec-24	09:00	09:00	-16.2433	42.4089	UW017	X	X	X	X			x	x	x	x
01-Dec-24	12:00	12:00	-16.5548	41.9586	UW018	X	X	X	X	x	x	x	x	x	x
01-Dec-24	15:00	15:00	-16.8868	41.4654	UW019	X	X	X	X			x	x	x	x

01-Dec-24	18:00	18:00	-17.1975	40.9989	UW020	X	X	X	X	x	x	x	x	x	x
02-Dec-24	06:00	06:00	-18.4648	39.0673	UW021	X	X	X	X	x	x		x	x	x
02-Dec-24	09:00	09:00	-18.7658	38.5986	UW022	X	X	X	X			x	x	x	x
02-Dec-24	12:00	12:00	-19.0303	38.1937	UW023	X	X	X	X	x	x	x	x	x	x
02-Dec-24	15:00	15:00	-19.2832	37.7934	UW024	X	X	X	X			x	x	x	x
02-Dec-24	18:00	18:00	-19.5684	37.34	UW025	X	X	X	X	x	x	x	x	x	x
03-Dec-24	06:00	06:00	-20.7979	35.3823	UW026	X	X	X	X	x	x		x	x	x
03-Dec-24	09:00	09:00	-21.1193	34.8501	UW027	X	X	X	X			x	x	x	x
03-Dec-24	12:00	12:00	-21.4096	34.3726	UW028	X	X	X	X	x	x	x	x	x	x
03-Dec-24	15:00	15:00	-21.71	33.8814	UW029	X	X	X	X			x	x	x	x
03-Dec-24	18:00	18:00	-21.955	33.473	UW030	X	X	X	X	x	x	x	x	x	x
04-Dec-24	06:00	06:00	-23.108	31.5426	UW031	X	X	X	X	x	x		x	x	x
04-Dec-24	09:00	09:00	-23.3963	31.0524	UW032	X	X	X	X			x	x	x	x
04-Dec-24	12:00	12:00	-23.6489	30.6155	UW033	X	X	X	X	x	x	x	x	x	x
04-Dec-24	15:00	15:00	-23.9321	30.1422	UW034	X	X	X	X			x	x	x	x
04-Dec-24	18:00	18:00	-24.2098	29.6973	UW035	X	X	X	X	x	x	x	x	x	x
05-Dec-24	06:00	06:00	-25.3158	27.9061	UW036	X	X	X	X	x	x		x	x	x
05-Dec-24	09:00	09:00	-25.6044	27.4369	UW037	X	X	X	X			x	x	x	x
05-Dec-24	12:00	12:00	-25.8637	27.0093	UW038	X	X	X		x	x	x	x	x	x
05-Dec-24	15:00	15:00	-26.1358	26.5635	UW039	X	X	X				x	x	x	x
05-Dec-24	18:00	18:00	-26.385	26.1433	UW040	X	X	X		x	x	x	x	x	x
06-Dec-24	06:00	06:00	-27.4453	24.3666	UW041	X	X	X		x	x		x	x	x
06-Dec-24	09:00	09:00	-27.723	23.8947	UW042		X	X				x	x	x	x
06-Dec-24	12:00	12:00	-27.9695	23.4854	UW043	X	X	X		x	x	x	x	x	x
06-Dec-24	15:00	15:00	-28.2301	23.0536	UW044		X	X				x	x	x	x
06-Dec-24	18:00	18:00	-28.3086	22.8748	UW045	X	X	X		x	x	x	x	x	x
07-Dec-24	06:00	06:00	-29.3455	21.134	UW046	X	X	X		x	x		x	x	x
07-Dec-24	09:00	09:00	-29.6125	20.6727	UW047		X	X				x	x	x	x
07-Dec-24	12:00	12:00	-29.8449	20.2676	UW048	X	X	X		x	x	x	x	x	x
07-Dec-24	15:00	15:00	-29.9528	19.8126	UW049		X	X				x	x	x	x
07-Dec-24	18:00	18:00	-29.8337	19.3707	UW050	X	X	X		x	x	x	x	x	x
08-Dec-24	06:00	06:00	-29.3346	17.4279	UW051	X	X	X		x	x		x	x	x
08-Dec-24	09:00	09:00	-29.2073	16.9263	UW052		X	X				x	x	x	x

08-Dec-24	12:00	12:00	-29.0865	16.4584	UW053	X	X	X		x	x	x	x	x	x
08-Dec-24	15:00	15:00	-28.9592	15.9548	UW054		X	X				x	x	x	x
08-Dec-24	18:00	18:00	-28.8388	15.4877	UW055	X	X	X		x	x	x	x	x	x
09-Dec-24	06:00	06:00	-28.3499	13.5424	UW056					x	x		x	x	x
09-Dec-24	09:00	09:00	-28.2224	13.0485	UW057							x	x	x	x
09-Dec-24	12:00	12:00	-28.1074	12.586	UW058					x	x	x	x	x	x
09-Dec-24	15:00	15:00	-27.981	12.0751	UW059		X	X				x	x	x	x
09-Dec-24	18:00	18:00	-27.8579	11.5904	UW060	X	X	X		x	x	x	x	x	x
10-Dec-24	06:00	06:00	-27.3473	9.5328	UW061	X	X	X		x	x		x	x	x
10-Dec-24	09:00	09:00	-27.2176	9.0103	UW062		X	X				x	x	x	x
10-Dec-24	12:00	12:00	-27.0981	8.5326	UW063	X	X	X				x	x	x	x
10-Dec-24	15:00	15:00	-26.9729	8.0216	UW064		X	X				x	x	x	x
10-Dec-24	18:00	18:00	-26.8651	7.5888	UW065	X	X	X		x	x	x	x	x	x
11-Dec-24	06:00	06:00	-26.3909	5.6695	UW066	X	X	X		x	x		x	x	x
11-Dec-24	09:00	09:00	-26.2963	5.3021	UW067		X	X				x	x	x	x
11-Dec-24	12:00	12:00	-26.2664	5.1768	UW068	X	X	X		x	x	x	x	x	x
11-Dec-24	15:00	15:00	-26.1503	4.6898	UW069		X	X				x	x	x	x
11-Dec-24	18:00	18:00	-26.0406	4.2394	UW070	X	X	X		x	x	x	x	x	x
12-Dec-24	06:00	06:00	-25.6107	2.4963	UW071					x	x		x	x	x
12-Dec-24	09:00	09:00	-25.5095	2.0713	UW072		X	X				x	x	x	x
12-Dec-24	12:00	12:00	-25.4088	1.6706	UW073	X	X	X		x	x	x	x	x	x
12-Dec-24	15:00	15:00	-25.2887	1.183	UW074							x	x	x	x
12-Dec-24	18:00	18:00	-25.1666	0.7185	UW075							x	x	x	x
13-Dec-24	06:00	06:00	-24.9968	-1.3317	UW076	X	X	X		x	x		x	x	x
13-Dec-24	09:00	09:00	-25.0024	-1.8596	UW077		X	X				x	x	x	x
13-Dec-24	12:00	12:00	-25	-2.3564	UW078	X	X	X		x	x	x	x	x	x
13-Dec-24	15:00	15:00	-25	-2.8897	UW079		X	X				x	x	x	x
13-Dec-24	18:00	18:00	-25	-3.3571	UW080	X	X	X		x	x	x	x	x	x
14-Dec-24	06:00	06:00	-24.9981	-5.6191	UW081	X	X	X		x	x		x	x	x
14-Dec-24	09:00	09:00	-24.9999	-6.1573	UW082		X	X				x	x	x	x
14-Dec-24	12:00	12:00	-25.0017	-6.6512	UW083	X	X	X		x	x	x	x	x	x
14-Dec-24	15:00	15:00	-25.0009	-7.1775	UW084		X	X				x	x	x	x
14-Dec-24	18:00	18:00	-25.0006	-7.6662	UW085	X	X	X		x	x	x	x	x	x

15-Dec-24	06:00	06:00	-25.001	-9.772	UW086					x	x		x	x		x
15-Dec-24	09:00	09:00	-25.0003	-10.3133	UW087							x	x	x		x
15-Dec-24	12:00	12:00	-25.0007	-10.8069	UW088	X	X	X		x	x	x	x	x		x
15-Dec-24	15:00	15:00	-24.9999	-11.3462	UW089							x	x	x		x
15-Dec-24	18:00	18:00	-24.9987	-11.8198	UW090					x	x	x	x	x		x
16-Dec-24	06:00	06:00	-25.0017	-13.9516	UW091	X	X	X		x	x		x	x		x
16-Dec-24	09:00	09:00	-25.003	-14.3509	UW092							x				
16-Dec-24	12:00	12:00	-24.8526	-14.4013	UW093							x				
16-Dec-24	15:00	15:00	-24.9864	-14.6724	UW094							x				
16-Dec-24	18:00	18:00	-24.9996	-15.1561	UW095	X	X	X		x	x	x	x	x		x
17-Dec-24	06:00	06:00	-25.001	-17.1568	UW096	X	X	X		x	x	x	x	x		x
17-Dec-24	09:00	09:00	-25.0025	-17.6775	UW097		X	X					x	x		x
17-Dec-24	12:00	12:00	-25.0007	-18.1576	UW098	X	X	X		x	x	x	x	x		x
17-Dec-24	15:00	15:00	-25.0023	-18.6386	UW099		X	X				x	x	x		x
17-Dec-24	18:00	18:00	-24.9993	-19.087	UW100	X	X	X		x	x	x	x	x		x
18-Dec-24	06:00	06:00	-25.0003	-20.9566	UW101	X	X	X		x	x	x	x	x		x
18-Dec-24	09:00	09:00	-25.0018	-21.4417	UW102		X	X					x	x		x
18-Dec-24	12:00	12:00	-25.0001	-21.9004	UW103	X	X	X		x	x	x	x	x		x
18-Dec-24	15:00	15:00	-25.0003	-22.4067	UW104		X	X				x	x	x		x
18-Dec-24	18:00	18:00	-24.9994	-22.8783	UW105	X	X	X		x	x	x	x	x		x
19-Dec-24	06:00	06:00	-24.9993	-25.0562	UW106	X	X	X		x	x	x	x	x		x
19-Dec-24	09:00	09:00	-25.0025	-25.57	UW107		X	X					x	x		x
19-Dec-24	12:00	12:00	-25.0006	-26.1027	UW108	X	X	X		x	x	x	x	x		x
19-Dec-24	15:00	15:00	-24.9979	-26.6916	UW109		X	X				x	x	x		x
19-Dec-24	18:00	18:00	-24.9996	-27.2164	UW110	X	X	X		x	x	x	x	x		x
20-Dec-24	06:00	06:00	-24.9993	-29.2858	UW111	X	X	X		x	x	x	x	x		x
20-Dec-24	09:00	09:00	-25.0043	-29.8253	UW112		X	X					x	x		x
20-Dec-24	12:00	12:00	-24.999	-30.2102	UW113	X	X	X		x	x	x	x	x		x
20-Dec-24	15:00	15:00	-25.0001	-30.6078	UW114		X	X				x	x	x		x
20-Dec-24	18:00	18:00	-25.0021	-30.9585	UW115	X	X	X		x	x	x	x	x		x
21-Dec-24	06:00	06:00	-25.0001	-32.5265	UW116	X	X	X	X	x	x	x	x	x		x
21-Dec-24	09:00	09:00	-24.9992	-32.9545	UW117		X	X	X				x	x		x
21-Dec-24	12:00	12:00	-24.9965	-33.4824	UW118	X	X	X	X	x	x	x	x	x		x

21-Dec-24	15:00	15:00	-24.9987	-34.0339	UW119		X	X	X			x	x	x	x
21-Dec-24	18:00	18:00	-24.999	-34.5223	UW120	X	X	X	X	x	x	x	x	x	x
22-Dec-24	06:00	06:00	-26.6772	-35.2325	UW121	X	X	X	X	x	x	x	x	x	x
22-Dec-24	09:00	09:00	-27.2223	-35.3059	UW122		X	X	X				x	x	x
22-Dec-24	12:00	12:00	-27.7519	-35.3767	UW123	X	X	X	X	x	x	x	x	x	x
22-Dec-24	15:00	15:00	-28.304	-35.4509	UW124		X	X	X			x	x	x	x
22-Dec-24	18:00	18:00	-28.857	-35.5306	UW125	X	X	X	X	x	x	x	x	x	x
23-Dec-24	06:00	06:00	-31.1941	-35.8495	UW126	X	X	X	X	x	x	x	x	x	x
23-Dec-24	09:00	09:00	-31.8049	-35.9317	UW127		X	X	X				x	x	x
23-Dec-24	12:00	12:00	-32.3276	-36.0025	UW128	X	X	X	X	x	x	x	x	x	x
23-Dec-24	15:00	15:00	-32.907	-36.0804	UW129		X	X	X			x	x	x	x
23-Dec-24	18:00	18:00	-33.4576	-36.1555	UW130	X	X	X	X	x	x	x	x	x	x
24-Dec-24	06:00	06:00	-35.9114	-36.4893	UW131	X	X	X	X	x	x	x	x	x	x
24-Dec-24	09:00	09:00	-36.5356	-36.5717	UW132		X	X	X				x	x	x
24-Dec-24	12:00	12:00	-37.1143	-36.6504	UW133	X	X	X	X	x	x	x	x	x	x
24-Dec-24	15:00	15:00	-37.751	-36.7349	UW134		X	X	X			x	x	x	x
24-Dec-24	18:00	18:00	-38.3195	-36.8135	UW135	X	X	X	X	x	x	x	x	x	x
25-Dec-24	06:00	06:00	-40.8289	-37.1499	UW136	X	X	X	X	x	x	x	x	x	x
25-Dec-24	09:00	09:00	-41.4012	-37.263	UW137		X	X	X				x	x	x
25-Dec-24	12:00	12:00	-41.8031	-37.3979	UW138	X	X	X	X	x	x	x	x	x	x
25-Dec-24	15:00	15:00	-41.8156	-37.4123	UW139		X	X	X				x	x	x
25-Dec-24	18:00	18:00	-42.1931	-37.5193	UW140	X	X	X	X	x	x	x	x	x	x
26-Dec-24	06:00	06:00	-44.8228	-38.3634	UW141	X	X	X	X	x	x		x	x	x
26-Dec-24	09:00	09:00	-45.4227	-38.5572	UW142		X	X	X			x	x	x	x
26-Dec-24	12:00	12:00	-46.0032	-38.7403	UW143	X	X	X	X	x	x	x	x	x	x
26-Dec-24	15:00	15:00	-46.6766	-38.9555	UW144		X	X	X			x	x	x	x
26-Dec-24	18:00	18:00	-47.2959	-39.1544	UW145	X	X	X	X	x	x	x	x	x	x
27-Dec-24	06:00	06:00	-49.7308	-39.9377	UW146	X	X	X	X	x	x		x	x	x
27-Dec-24	09:00	09:00	-50.1859	-39.738	UW147		X	X	X			x	x	x	x
27-Dec-24	12:00	12:00	-50.5548	-39.3687	UW148	X	X	X	X	x	x	x	x	x	x
27-Dec-24	15:00	15:00	-50.959	-38.9616	UW149		X	X	X			x	x	x	x
27-Dec-24	18:00	18:00	-51.3121	-38.6036	UW150	X	X	X	X	x	x	x	x	x	x

Appendix 2 - Argo Float Deployments.

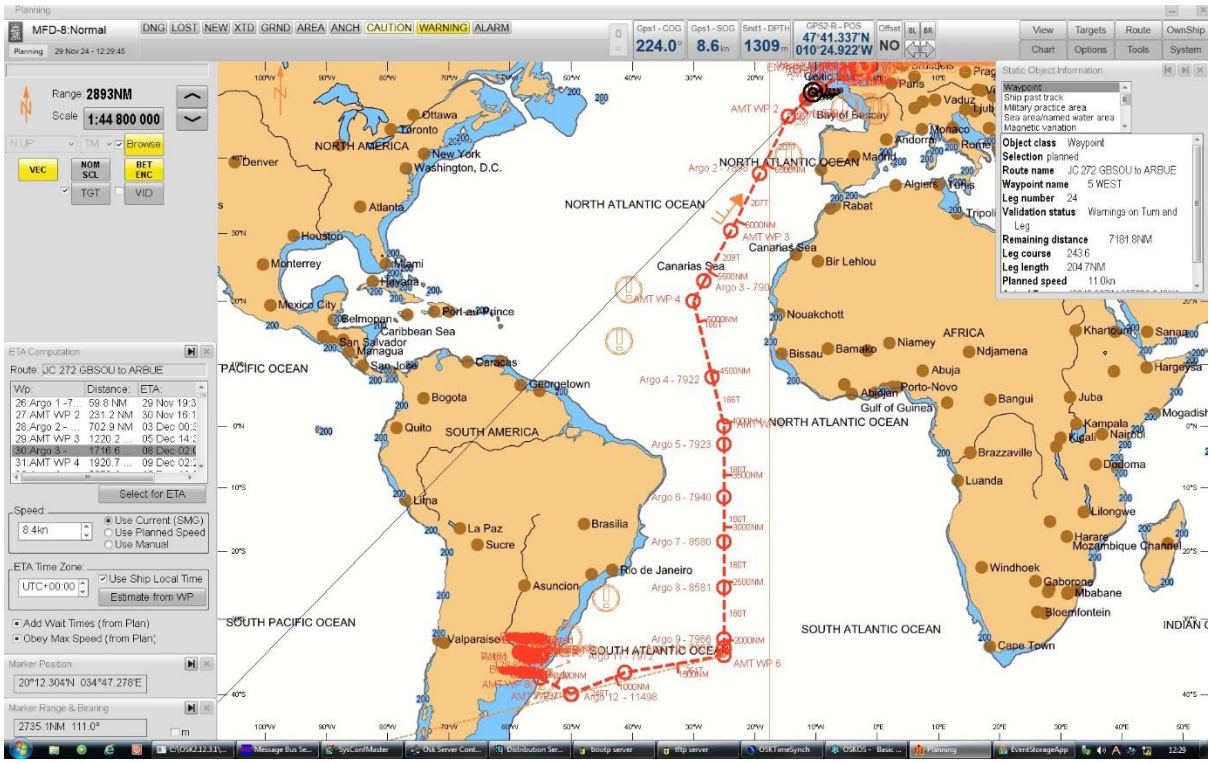

****

Deployment log of Float Serial# 7794.

Float Type: WHOI Core**

Ship: RRS James Cook,

Cruise Name: JC272,

Start-up Operator: Kat Parise.

Magnetic swipe start-up: 29-10-2024.

Deployment Operator: Gavin Tilstone.

Deployment Date: 29-11-2024.

Deployment Time: 19:36:47.

Deployment Latitude: 47.00525 N,

Deployment Longitude: -11.469689 W.

Deployment Type: Boxed.

Deployment Method: Sling method.

Deployment position: Stern.

Ship Speed: 1.2 knots.

Beaufort scale: 5.

Wind speed: 20 knots.

Bathymetry depth: 4754 m.

Additional Comments: Water release failed, hence sling method deployed.

****

Deployment log of Float Serial# 7898.

Float Type: WHOI Core

Ship: RRS James Cook,

Cruise Name: JC272,

Start-up Operator: Kat Parise.

Magnetic swipe start-up: 29-10-2024.

Deployment Operator: Gavin Tilstone.

Deployment Date: 02-12-2024.

Deployment Time: 14:31.

Deployment Latitude: 38.005681 N,

Deployment Longitude: -19.146014 W.

Deployment Type: Boxed.

Deployment Method: Sling method.

Deployment position: Stern.

Ship Speed: 1.7 knots.

Beaufort scale: 4.

Wind speed: 11 knots.

Sea state: 2.1 m

Bathymetry depth: 5100 m.

Additional Comments: Water release failed on #7794, so will use sling method for deployment from now on.

****

Deployment log of Float Serial# 7900.

Float Type: WHOI Core

Ship: RRS James Cook,

Cruise Name: JC272,

Start-up Operator: Kat Parise.

Magnetic swipe start-up: 29-10-2024.

Deployment Operator: Gavin Tilstone.

Deployment Date: 06-12-2024.

Deployment Time: 16:30.

Deployment Latitude: 23.005007 N,

Deployment Longitude: -28.258729 W.

Deployment Type: Boxed.

Deployment Method: Sling method.

Deployment position: Stern.

Ship Speed: 0.6 knots.

Beaufort scale: 5.

Wind speed: 10 m/s.

Bathymetry depth: 5570 m.

Additional Comments: Water release failed on #7794, so we are using the sling method for deployment from now on.

****

Deployment log of Float Serial# 7922:

Float Type: WHOI Core

Ship: RRS James Cook,

Cruise Name: JC272,

Start-up Operator: Kat Parise.

Magnetic swipe start-up: 29-10-2024.

Deployment Operator: Gavin Tilstone.

Deployment Date: 10-12-2024.

Deployment Time: 16:10.

Deployment Latitude: 08.005791 N,

Deployment Longitude: -26.969327 W.

Deployment Type: Boxed.

Deployment Method: Sling method.

Deployment position: Stern.

Ship Speed: 1.4 knots.

Sea state: 1.7 m

Wind speed: 7.64 knots.

Bathymetry depth: 5075 m.

Additional Comments: Water release failed on previous floats; sling method deployed as default.

****

Deployment log of Float Serial# 7923:

Float Type: WHOI Core

Ship: RRS James Cook,

Cruise Name: JC272,

Start-up Operator: Kat Parise.

Magnetic swipe start-up: 29-10-2024.

Deployment Operator: Gavin Tilstone.

Deployment Date: 13-12-2024.

Deployment Time: 16:47.

Deployment Latitude: -08.00216 S,

Deployment Longitude: -24.998043 W.

Deployment Type: Boxed.

Deployment Method: Sling method.

Deployment position: Stern.

Ship Speed: 1.4 knots.

Beaufort scale: 4 m

Wind speed: 6.24 knots.

Bathymetry depth: 5328 m.

Additional Comments: Water release failed on previous floats; sling method deployed as default.

****

Deployment log of Float Serial# 7940:

Float Type: WHOI Core

Ship: RRS James Cook,

Cruise Name: JC272,

Start-up Operator: Kat Parise.

Magnetic swipe start-up: 29-10-2024.

Deployment Operator: Gavin Tilstone.

Deployment Date: 15-12-2024.

Deployment Time: 17:58.

Deployment Latitude: -11.495931 S,

Deployment Longitude: -24.998254 W.

Deployment Type: Boxed.

Deployment Method: Sling method.

Deployment position: Stern.

Ship Speed: 1.4 knots.

Beaufort scale: 4

Wind speed: 6.06 knots.

Bathymetry depth: 4288 m.

Additional Comments: Water release failed on previous floats; sling method deployed as default.

****

Deployment log of Float Serial# 8580:

Float Type: UK Core***

Ship: RRS James Cook,

Cruise Name: JC272,

Start-up Operator: ??

Magnetic swipe start-up: ??-??-2024.

Deployment Operator: Gavin Tilstone.

Deployment Date: 17-12-2024.

Deployment Time: 16:03.

Deployment Latitude: -18.500065 S,

Deployment Longitude: -24.998367 W.

Deployment Type: Lowered.

Deployment Method: Rope through plastic damper.

Deployment position: Stern.

Ship Speed: 1.3 knots.

Beaufort scale: 4.

Wind speed: 8.45 m/s.

Bathymetry depth: 5535 m.

Additional Comments: None.

****

Deployment log of Float Serial# 8581:

Float Type: UK Core

Ship: RRS James Cook,

Cruise Name: JC272,

Start-up Operator: ??

Magnetic swipe start-up: ??-??-2024.

Deployment Operator: Gavin Tilstone.

Deployment Date: 19-12-2024.

Deployment Time: 10:333.

Deployment Latitude: -25.498326 S,

Deployment Longitude: -25.001562 W.

Deployment Type: Lowered from crane.

Deployment Method: Rope through plastic damper.

Deployment position: Stern.

Ship Speed: 1.5 knots.

Beaufort scale: 3.

Wind speed: ?? m/s.

Bathymetry depth: 4996 m.

Additional Comments: None.

****

Deployment log of Float Serial# 7966:

Float Type: WHOI Core

Ship: RRS James Cook,

Cruise Name: JC272,

Start-up Operator: Kat Parise.

Magnetic swipe start-up: 29-10-2024.

Deployment Operator: Gavin Tilstone.

Deployment Date: 21-12-2024.

Deployment Time: 04:59.

Deployment Latitude: -32.79435 S,

Deployment Longitude: -25.001203 W.

Deployment Type: Boxed.

Deployment Method: Sling method.

Deployment position: Stern.

Ship Speed: 2.0 knots.

Beaufort scale: 3

Wind speed: 7.34 knots.

Bathymetry depth: 4381 m.

Additional Comments: Water release failed on previous floats; sling method deployed as default.

****

Deployment log of Float Serial# 7972:

Float Type: WHOI Core

Ship: RRS James Cook,

Cruise Name: JC272,

Start-up Operator: Kat Parise.

Magnetic swipe start-up: 29-10-2024.

Deployment Operator: Gavin Tilstone.

Deployment Date: 25-12-2024.

Deployment Time: 09:56.

Deployment Latitude: -37.199894 S,

Deployment Longitude: -41.206457 W.

Deployment Type: Boxed.

Deployment Method: Sling method.

Deployment position: Stern.

Ship Speed: 0.9 knots.

Beaufort scale: 4

Wind speed: 9.28 knots.

Bathymetry depth: 4980 m.

Additional Comments: Water release failed on previous floats; sling method deployed as default.

****

Deployment log of Float Serial# 11498:

Float Type: WHOI Core

Ship: RRS James Cook,

Cruise Name: JC272,

Start-up Operator: Kat Parise.

Magnetic swipe start-up: 29-10-2024.

Deployment Operator: Gavin Tilstone.

Deployment Date: 27-12-2024.

Deployment Time: 08:58 UTC.

Deployment Latitude: -39.999789 S,

Deployment Longitude: -49.925499 W.

Deployment Type: Boxed.

Deployment Method: Sling method.

Deployment position: Stern.

Ship Speed: 2 knots.

Beaufort scale: 4

Wind speed: 9.02 knots.

Bathymetry depth: 5410 m.

Additional Comments: Water release failed on previous floats; sling method deployed as default.